AD-A175 200 ON THE FRACTURE STRESS FOR THE INCLINED CRACK UNDER BIAXIAL LOAD(U) NAVAL RESEARCH LAB WASHINGTON DC J EFTIS ET AL 14 NOV 86 NRL-MR-5876 1/1

UNCLASSIFIED F/G 20/11 NL

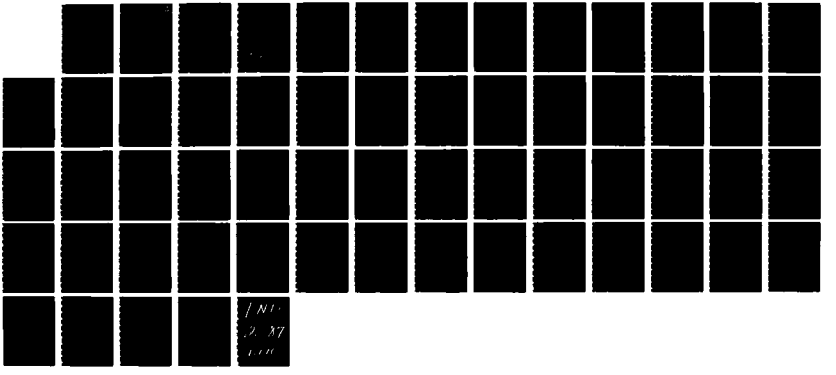

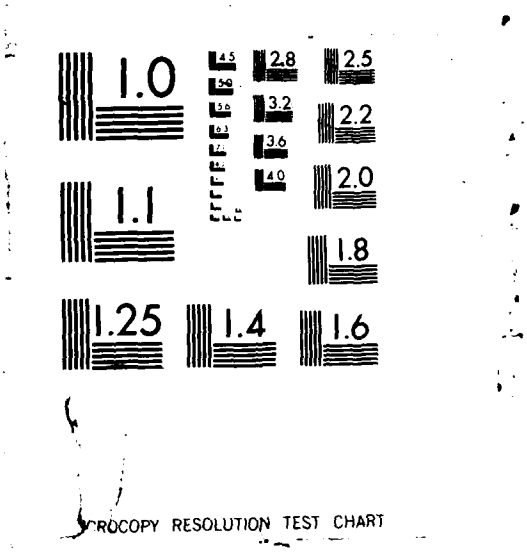
1.0
1.1
1.25
1.4
1.6
1.8
2.0
2.2
2.5
2.8
3.2
3.6
4.0
4.5
5.0
ROCOPY RESOLUTION TEST CHART

On the Fracture Stress for the Inclined Crack Under Biaxial Load

JOHN EFTIS* AND MITCHELL I. JOLLES

Mechanics of Materials Branch
Material Science and Technology Division

**Geo-Centers, Inc.*
Suitland, MD 20746

AD-A175200

SECURITY CLASSIFICATION OF THIS PAGE

REPORT DOCUMENTATION PAGE

1a. REPORT SECURITY CLASSIFICATION UNCLASSIFIED	1b. RESTRICTIVE MARKINGS
2a. SECURITY CLASSIFICATION AUTHORITY	3. DISTRIBUTION / AVAILABILITY OF REPORT Approved for public release; distribution unlimited.
2b. DECLASSIFICATION / DOWNGRADING SCHEDULE	
4. PERFORMING ORGANIZATION REPORT NUMBER(S) NRL Memorandum Report 5876	5. MONITORING ORGANIZATION REPORT NUMBER(S)
6a. NAME OF PERFORMING ORGANIZATION Naval Research Laboratory 6b. OFFICE SYMBOL (If applicable) Code 6382	7a. NAME OF MONITORING ORGANIZATION
6c. ADDRESS (City, State, and ZIP Code) Washington, DC 20375-5000	7b. ADDRESS (City, State, and ZIP Code)
8a. NAME OF FUNDING / SPONSORING ORGANIZATION Office of Naval Research 8b. OFFICE SYMBOL (If applicable)	9. PROCUREMENT INSTRUMENT IDENTIFICATION NUMBER
8c. ADDRESS (City, State, and ZIP Code) Arlington, VA 22217	10. SOURCE OF FUNDING NUMBERS PROGRAM ELEMENT NO. 61153N22 / PROJECT NO. RR022-01-48 / TASK NO. / WORK UNIT ACCESSION NO. DN480-509

11. TITLE (Include Security Classification)
On the Fracture Stress for the Inclined Crack Under Biaxial Load

12. PERSONAL AUTHOR(S)
Eftis, John* and Jolles, Mitchell I.

13a. TYPE OF REPORT	13b. TIME COVERED FROM ____ TO ____	14. DATE OF REPORT (Year, Month, Day)	15. PAGE COUNT
		1986 November 14	59

16. SUPPLEMENTARY NOTATION
*Geo Centers, Inc., Suitland, MD 20746

17. COSATI CODES			18. SUBJECT TERMS (Continue on reverse if necessary and identify by block number)
FIELD	GROUP	SUB-GROUP	
			Fracture mechanics

19. ABSTRACT (Continue on reverse if necessary and identify by block number)

The tensile vertical load required to fracture a biaxially loaded plane infinite sheet (in plane stress or plane strain) with an inclined crack is determined using the Griffith fracture criterion. The infinite plane geometry is used as a prototype enabling analytical demonstration of the qualitative features of the problem, such as the dependence of the critical load on the load biaxiality, crack orientation and Poisson's ratio of the material. Existing experimental data for a horizontal crack are summarized and found qualitatively in agreement with the results of the analysis.

20. DISTRIBUTION / AVAILABILITY OF ABSTRACT ☒ UNCLASSIFIED/UNLIMITED ☐ SAME AS RPT ☐ DTIC USERS	21. ABSTRACT SECURITY CLASSIFICATION UNCLASSIFIED
22a. NAME OF RESPONSIBLE INDIVIDUAL Mitchell I. Jolles	22b. TELEPHONE (Include Area Code) (202) 767-6451 22c. OFFICE SYMBOL Code 6382

DD FORM 1473, 84 MAR 83 APR edition may be used until exhausted. All other editions are obsolete.

SECURITY CLASSIFICATION OF THIS PAGE

CONTENTS

1. INTRODUCTION 1

2. ANALYTICAL SOLUTION 5

3. POWER SERIES REPRESENTATION OF THE STRESS AND DISPLACEMENT FIELDS 5

4. GRIFFITH CRACK INSTABILITY CRITERION 7

5. CALCULATION OF THE ELASTIC STRAIN ENERGY DERIVATIVE 10

6. THE CRITICAL OR FRACTURE LOAD 17

7. FRACTURE STRESS TEST DATA FOR THE HORIZONTALLY ORIENTED CRACK 21

8. CONCLUSIONS 26

ACKNOWLEDGMENT 27

REFERENCES 28

NOMENCLATURE

$(x,y),(x',y'),(r,\theta)$	=	rectangular and polar coordinates, respectively.
z	=	$x+iy=re^{i\theta}$, complex variable.
t_{jk}, e_{jk}	=	components of the stress and strain tensors, respectively.
T_k, u_k, b_k	=	components of the surface traction, displacement and body force vectors, respectively.
t_{xx}, t_{xy}, t_{yy}	=	rectangular stress components.
u_x, u_y	=	rectangular displacement components.
$2a$	=	crack dimension.
α	=	crack inclination.
k	=	applied load biaxiality ratio, $t_{xx}(\infty)/t_{yy}(\infty)$.
σ	=	uniform stress applied to the outer boundary surface.
μ	=	elastic shear modulus.
E	=	Young's elastic modulus.
ν	=	Poisson's ratio.
κ	=	$(3-\nu)/(1+\nu)$ for plane stress, $(3-4\nu)$ for plane strain.
γ	=	surface density per unit area.
U	=	elastic strain energy density per unit thickness.
W	=	work of forces applied to the body.
P,V	=	the potential energy of the system and the elastic potential energy, respectively.
Γ	=	surface energy.
R	=	bound region of the x-y plane.
Λ_k	=	closed boundary curves of R.
Φ,Ω,ϕ,ω	=	holomorphic functions of the complex variable z.

ON THE FRACTURE STRESS FOR THE INCLINED CRACK UNDER BIAXIAL LOAD

1. Introduction

The significance of load biaxiality for fracture was investigated initially for the horizontal crack [1], and then for the inclined crack [2]. Attention in each of these studies was confined to analysis of the local region enclosing the crack-tip. Calculation of the critical (fracture) stress under biaxial applied load, in which the Griffith crack instability hypothesis was utilized, then followed for the horizontal single crack and for horizontally oriented collinear cracks [3,4]. A similar type of calculation was also performed for the so-called 'shear panel' [5].

In this paper the value of the tensile vertical load necessary to fracture a biaxially loaded plane infinite sheet (in plane stress or plane strain) with an inclined crack is determined using the Griffith fracture criterion. The infinite plane geometry is used initially as a prototype enabling analytical demonstration of the qualitative features of the problem as, for example, the interplay of the dependence of the critical tensile load, σ_c, on the load biaxiality, the crack orientation and the Poisson ratio for the material.

A similar calculation for σ_c for a plane body having finite dimensions and an inclined central crack using the finite element method, is to follow for comparative purposes.

Experimental data from several biaxial load fracture test programs, [6-9], using horizontally oriented cracks, encompassing three different kinds of structural materials, are summerized here. This data provides some measure of corroboration of the qualitative features of the dependence of the critical tensile load upon the load biaxiality and the material Poisson ratio as indicated by the prototype analysis.

Manuscript approved October 3, 1986.

2. Analytical Solution

The stress boundary conditions of the plane infinite cracked-body shown in Fig. 1 are, relative to the (x'-y') coordinate system,

$$t'_{yy} = \sigma \ , \quad t'_{xx} = k\sigma \ , \quad t'_{xy} = 0 \qquad \text{as } |z| \to \infty \ , \tag{2.1}$$

whereas relative to the (x-y) coordinate system they become

$$\begin{aligned} t_{xx} &= \tfrac{1}{2}\sigma(1+k) - \tfrac{1}{2}\sigma(1-k)\cos 2\alpha \\ t_{yy} &= \tfrac{1}{2}\sigma(1+k) + \tfrac{1}{2}\sigma(1-k)\cos 2\alpha \qquad \text{as } |z| \to \infty \\ t_{xy} &= \tfrac{1}{2}\sigma(1-k)\sin 2\alpha \ . \end{aligned} \tag{2.2}$$

Along the interior crack border

$$t_{yy}(x,0) = t_{xy}(x,0) = 0 \ , \qquad |x| < |a| \ . \tag{2.3}$$

As a problem of plane linear elasticity, the formal unique solution of the boundary value problem posed by Fig. 1 is expressed in terms of the following sectionally holomorphic functions of the complex variable $z = x + iy = re^{i\theta}$ [10],

$$\begin{aligned} \Phi(z) &= \frac{C_1 z}{(z^2-a^2)^{\frac{1}{2}}} - C_2 \\ \Omega(z) &= \frac{C_1 z}{(z^2-a^2)^{\frac{1}{2}}} + C_2 \ , \end{aligned} \tag{2.4}$$

where

$$\begin{aligned} C_1 &= \tfrac{\sigma}{4}[(1-e^{2i\alpha})+k(1+e^{2i\alpha})] = \tfrac{\sigma}{4}(1+k) - \tfrac{\sigma}{4}(1-k)[\cos 2\alpha + i \sin 2\alpha] \\ C_2 &= -\tfrac{\sigma}{4}(1-k)e^{2i\alpha} = -\tfrac{\sigma}{4}(1-k)[\cos 2\alpha + i \sin 2\alpha] \ . \end{aligned} \tag{2.5}$$

Needed in the sequel are the integrals of $\Phi(z)$ and $\Omega(z)$, (expressed to within negligible arbitrary complex constants that contribute only to rigid body displacements),

$$\phi(z) = \int \Phi(z)dz = C_1(z^2-a^2)^{\frac{1}{2}} - C_2 z$$

$$\omega(z) = \int \Omega(z)dz = C_1(z^2-a^2)^{\frac{1}{2}} + C_2 z \ . \tag{2.6}$$

Also needed is the notational convention for conjugation of arguments of functions, values of functions and, also, of their derivatives. Thus if $\bar{z} = x - iy$ and

$$\psi(z) = f_1(x,y) + if_2(x,-y) \quad ,$$

then

$$\psi(\bar{z}) = f_1(x,-y) + if_2(x,-y)$$

$$\bar{\psi}(z) = f_1(x,y) - if_2(x,y)$$

$$\bar{\psi}(\bar{z}) = \overline{\psi(z)} = f_1(x,-y) - if_2(x,-y) \tag{2.7}$$

$$\psi'(z) = \frac{d\psi}{dz}(z) \quad , \quad \psi'(\bar{z}) = \frac{d\psi}{d\bar{z}}(\bar{z})$$

$$\overline{\psi'(z)} = \frac{d\bar{\psi}}{dz}(z) \quad , \quad \overline{\psi'(z)} = \frac{d\bar{\psi}}{d\bar{z}}(\bar{z}) \quad .$$

The stress and displacement components are determined from the solution expressions (2.4)-(2.6) by set of relations

$$t_{xx} + t_{yy} = 2[\Phi(z) + \overline{\Phi(z)}] = 4\mathrm{Re}[\Phi(z)]$$

$$t_{xx} - it_{xy} = \Phi(z) + \Omega(\bar{z}) + (z-\bar{z})\overline{\Phi'(z)} \tag{2.8}$$

$$2\mu(u_x + iu_y) = \kappa\phi(z) - \omega(\bar{z}) - (z-\bar{z})\overline{\Phi(z)} \quad .$$

It will be more convenient to have expressions (2.8) in the following uncoupled form:

$$
\begin{aligned}
t_{yy} &= \mathrm{Re}[\phi(z)] + 2y\,\mathrm{Im}[\phi'(z)] + \mathrm{Re}[\bar{\Omega}(z)] \\
t_{xx} &= 3\mathrm{Re}[\phi(z)] - 2y\,\mathrm{Im}[\phi'(z)] - \mathrm{Re}[\Omega(\bar{z})] \\
t_{xy} &= -2y\mathrm{Re}[\phi'(z)] + \mathrm{Im}[\bar{\Omega}(z)] - \mathrm{Im}[\phi(z)] \qquad (2.9) \\
2\mu u_x &= \kappa\mathrm{Re}[\phi(z)] - \mathrm{Re}[\omega(\bar{z})] - 2y\,\mathrm{Im}[\phi(z)] \\
2\mu u_y &= \kappa\mathrm{Im}[\phi(z)] - \mathrm{Im}[\omega(\bar{z})] - 2y\,\mathrm{Re}[\phi(z)] \quad .
\end{aligned}
$$

Expressions (2.4)-(2.6), together with equations (2.9), are sufficient to determine uniquely the stress and displacement fields at every interior point of the biaxially loaded infinite cracked-body having the geometry illustrated by Fig. 1.

3. Power Series Representation of the Stress and Displacement Fields

Needed for the subsequent calculation of the elastic strain energy of the body are the power series representations for the stress and displacement components. Consequently the analytic functions $\phi(z)$, $\phi'(z)$, $\Omega(\bar{z})$, $\bar{\Omega}(z)$, $\psi(z)$ and $\omega(\bar{z})$ appearing in the uncoupled stress-displacement equations (2.9) are expanded about the origin as power (Taylor) series as follows. For $(a/|z|) < 1$,

$$\phi(z) = (C_1-C_2)+C_1\left\{\frac{1}{2}\left(\frac{a}{z}\right)^2+\frac{3}{8}\left(\frac{a}{z}\right)^4+\frac{5}{16}\left(\frac{a}{z}\right)^6+\cdots\right\}$$

$$\phi'(z) = -C_1\left\{\frac{a^2}{z^3}+\frac{3}{2}\frac{a^4}{z^5}+\frac{15}{8}\frac{a^6}{z^7}+\cdots\right\}$$

$$\Omega(\bar{z}) = (C_1+C_2)+\bar{C}_1\left\{\frac{1}{2}\left(\frac{a}{\bar{z}}\right)^2+\frac{3}{8}\left(\frac{a}{\bar{z}}\right)^4+\frac{5}{16}\left(\frac{a}{\bar{z}}\right)^6+\cdots\right\} \qquad (3.1)$$

$$\bar{\Omega}(z) = (\bar{C}_1+\bar{C}_2)+C_1\left\{\frac{1}{2}\left(\frac{a}{z}\right)^2+\frac{3}{8}\left(\frac{a}{z}\right)^4+\frac{5}{16}\left(\frac{a}{z}\right)^6+\cdots\right\}$$

$$\psi(z) = (C_1-C_2)z-C_1\left\{\frac{1}{2}\left(\frac{a^2}{z}\right)+\frac{1}{8}\left(\frac{a^4}{z^3}\right)+\frac{1}{16}\left(\frac{a^6}{z^5}\right)+\cdots\right\}$$

$$\omega(\bar{z}) = (C_1+C_2)\bar{z}-C_1\left\{\frac{1}{2}\left(\frac{a^2}{\bar{z}}\right)+\frac{1}{8}\left(\frac{a^4}{\bar{z}^3}\right)+\frac{1}{16}\left(\frac{a^6}{\bar{z}^5}\right)+\cdots\right\}.$$

After conversion into the polar coordinates (r,ϑ), the series (3.1) when substituted into Eqs. (2.9) produce the following series expressions for the stress and displacements in the large, i.e., for all points (r,ϑ) for which $r > a$.

$$t_{yy} = 2C_1^R + \left\{\left(\frac{a}{r}\right)^2 [C_1^R(\cos 2\theta + 2\sin\theta\sin 3\theta) - C_1^I(2\sin\theta\cos 3\theta)]\right.$$
$$\left. + \left(\frac{a}{r}\right)^4 [C_1^R(\frac{3}{4}\cos 4\theta + 3\sin\theta\sin 5\theta) - C_1^I(3\sin\theta\cos 5\theta)] + \mathcal{O}\left(\frac{a}{r}\right)^6\right\}$$

$$t_{xx} = 3(C_1-C_2)^R - (C_1+C_2)^R + \left\{\left(\frac{a}{r}\right)^2 [C_1(\cos 2\theta - 2\sin\theta\sin 3\theta) + C_1^I(2\sin 2\theta + 2\sin\theta\cos 3\theta)]\right. \quad (3.2)$$
$$\left. + \left(\frac{a}{r}\right)^4 [C_1^R(\frac{3}{4}\cos 4\theta - 3\sin\theta\sin 5\theta) + C_1^I(\frac{3}{2}\sin 4\theta + 3\sin\theta\cos 5\theta)] + \mathcal{O}\left(\frac{a}{r}\right)^6\right\}$$

$$t_{xy} = -2C_1^I + \left\{\left(\frac{a}{r}\right)^2 [C_1^I(2\sin\theta\sin 3\theta - \cos 2\theta) + C_1^R(2\sin\theta\cos 3\theta)]\right.$$
$$\left. + \left(\frac{a}{r}\right)^4 [C_1^I(3\sin\theta\sin 5\theta - \frac{3}{4}\cos 4\theta) + C_1^R(3\sin\theta\cos 5\theta)] + \mathcal{O}\left(\frac{a}{r}\right)^6\right\},$$

and

$$2\mu u_x = \left\{\left(\frac{a^2}{r}\right)[C_1^R\left\langle\frac{(1-\kappa)}{2}\cos\theta + \sin\theta\sin 2\theta\right\rangle - C_1^I\left\langle\frac{(1+\kappa)}{2}\sin\theta + \sin\theta\cos 2\theta\right\rangle]\right.$$
$$+ \left(\frac{a^4}{r^3}\right)[C_1^R\left\langle\frac{(1-\kappa)}{8}\cos 3\theta + \frac{3}{4}\sin\theta\sin 4\theta\right\rangle - C_1^I\left\langle\frac{(1+\kappa)}{8}\sin 3\theta + \frac{3}{4}\sin\theta\cos 4\theta\right\rangle]$$
$$\left. + \mathcal{O}\left(\frac{a^6}{r^5}\right)\right\} + \frac{\sigma}{4}\left\{(\kappa-1)(1+k)r\cos\theta + 2(1-k)r(\cos\theta\cos 2\alpha + \sin\theta\sin 2\alpha)\right\} \quad (3.3)$$

$$2\mu u_y = \left\{\left(\frac{a^2}{r}\right)[C_1^I\left\langle\frac{(1-\kappa)}{2}\cos\theta - \sin\theta\sin 2\theta\right\rangle + C_1^R\left\langle\frac{(1+\kappa)}{2}\sin\theta - \sin\theta\cos 2\theta\right\rangle]\right.$$
$$+ \left(\frac{a^4}{r^3}\right)[C_1^I\left\langle\frac{(1-\kappa)}{8}\cos 3\theta - \frac{3}{4}\sin\theta\sin 4\theta\right\rangle + C_1^R\left\langle\frac{(1+\kappa)}{8}\sin 3\theta - \frac{3}{4}\sin\theta\cos 4\theta\right\rangle]$$
$$\left. + \mathcal{O}\left(\frac{a^6}{r^5}\right)\right\} + \frac{\sigma}{4}(1+k)(\kappa-1)r\sin\theta + \frac{\sigma}{2}(1-k)[r\cos\theta\sin 2\alpha - r\sin\theta\cos 2\alpha] .$$

In these equations

$$C_1^R = \frac{\sigma}{4}[(1+k)-(1-k)\cos 2\alpha]$$
$$C_1^I = -\frac{\sigma}{4}(1-k)\sin 2\alpha \quad (3.4)$$
$$(C_1-C_2)^R = \frac{\sigma}{4}(1+k) \quad ; \quad (C_1+C_2)^R = \frac{\sigma}{4}(1+k) - \frac{\sigma}{2}(1-k)\cos 2\alpha$$
$$3(C_1-C_2)^R - (C_1+C_2)^R = \frac{\sigma}{2}(1+k) + \frac{\sigma}{2}(1-k)\cos 2\alpha .$$

4. Griffith Crack Instability Criterion

The criterion for crack instability, or fracture, introduced by Griffith [9 ,11] requires that at the onset of fracture, meaning here rapid crack propagation, the potential energy of the system, P, must acquire a stationary (maximum) value. The necessary condition that this be so is

$$\frac{dP}{da} = 0 \quad . \tag{4.1}$$

For a body with elastic material behavior, the total potential energy of the system consists of the crack surface energy, Γ, and the elastic potential energy, V. The latter is the difference between the elastic strain energy, U, and the work (energy) of the applied boundary tractions and body force in bringing the body to its deformed equilibrium configuration. Thus

$$P = V + \Gamma \ , \tag{4.2}$$

where

$$V = \int_R \frac{1}{2} t_{jk} e_{jk} dV - \left(\int_S T_k u_k dA + \int_R b_k u_k dV \right) \ , \quad j,k=1,2,3. \tag{4.3}$$

The T_κ are the traction components applied over the surface S bounding the region R of the body, which is also subject to the body force components b_κ. The u_κ are the displacement components. The linear elastic strain energy of the deformed body is

$$U = \int_R \frac{1}{2} t_{jk} e_{jk} dV \quad , \tag{4.4}$$

where t_{jk} and e_{jk} are the stress and infinitesimal strain components, respectively.

An application of Clapeyron's theorem [12], which states that

$$\int_S T_k u_k dA + \int_R b_k u_k dV = 2U \quad , \tag{4.5}$$

allows the potential energy of the system to be expressed equivalently as

$$P = \Gamma - U \quad . \tag{4.6}$$

The condition for onset of fracture thus becomes

$$\frac{d}{da} (\Gamma - U) = 0 \quad . \tag{4.7}$$

Since Griffith assumes that the crack surface energy is equal to the crack surface area multiplied by a constant surface energy density, γ, application of the fracture criterion (4.7) reduces to a calculation of the derivative of the elastic strain energy of the entire body.

At the risk of appearing somewhat pedantic, the author believes that it might prove useful at this juncture to offer several observations with respect to the fracture criterion (4.1) or (4.7). Application of the Griffith criterion does not in any way imply the subsequent direction of crack propagation, be it at some angle with respect to the plane of the original crack, or along the direction of the original crack. There is nothing within the criterion that can allow for this. The operation of performing the elastic strain energy derivative dU/da, by the definition of derivative, requires the use of two incrementally differing crack sizes, for the same crack geometry and loading, in the limit as the increment goes to zero. This operation does not suggest that when fracture ensues the subsequent crack extension must be along the original direction of the plane of the crack. What it does provide is the value of the rate of change of the elastic

strain energy of the entire body with respect to change of crack length when the crack has its original size. Nothing more is stated or implied.

Another point of interest deserves comment. Were the elastic energy derivative to have the value zero, then the fracture criterion, as expressed in the form given by Eq. (4.7), would lose its applicability. Is it physically possible for dU/da to have the value zero? We know from compliance type calculations that the elastic strain energy derivative can be positive valued or negative valued under 'dead load' or 'fixed grips' boundary constraints, respectively. If, furthermore, the derivative itself is a continuous function of the crack length, then it must also have the possibility of having a zero value as well. It is physically plausible to imagine that this can occur if the rate of the elastic strain energy increase with change of crack size associated with the deformation of the body near the outer boundary, is just equal to the rate of elastic strain energy decrease (release) associated with the relaxation of strains around the crack.

5. Calculation of the Elastic Strain Energy Derivative

Let U and U' denote the elastic strain energy of the infinite body when the crack dimensions of the body are 2a and 2a', respectively, where the difference $\Delta a = (a'-a)$ is arbitrarily small and the crack geometry and the boundary tractions are the same for each of the crack lengths. The required strain energy derivative may be determined either by means of a defining limit type of calculation

$$\lim_{(a'-a)\to 0} \left(\frac{U'-U}{a'-a}\right) = \frac{dU}{da} \quad , \tag{5.1}$$

or by formal differentiation of U. Both types of calculation have been previously shown and discussed for the horizontal crack geometry [3,4,5]. Therefore only the latter of the two methods will be employed here since it is the simpler of the two.

Referring to Fig. 2, the elastic strain energy (per unit thickness) of the plane region R, bound by the simple closed boundary curves Λ_1 and Λ_2, is given by the integral

$$U(R) = \frac{1}{2} \int\int_R \left[t_{xx} \frac{\partial u_x}{\partial x} + t_{yy} \frac{\partial u_y}{\partial y} + t_{xy} \left(\frac{\partial u_x}{\partial y} + \frac{\partial u_y}{\partial x} \right) \right] dxdy \quad . \tag{5.2}$$

By means of Green's theorem for a doubly connected domain [13] this multiple integral over the region R can be transformed into line integrals about the bounding contours Λ_1 and Λ_2 as

$$\begin{aligned} U(R) &= I(\Lambda_1) + I(\Lambda_2) \\ &= \frac{1}{2} \left(\oint_{\Lambda_1} + \oint_{\Lambda_2} \right) ([t_{xx}u_x + t_{xy}u_y]dy - [t_{yy}u_y + t_{xy}u_x]dx) \quad . \end{aligned} \tag{5.3}$$

Other than being simple (non-self intersecting) nested closed curves that enclose the crack, Λ_1 and Λ_2 are arbitrary otherwise. For convenience they may be chosen such that Λ_1 is a circle of radius $r_0 > |a|$ centered at the origin of the coordinates, while Λ_2 coincides with the borders of the crack [cf. Fig. 3]. Since line integration along the crack borders require that dy be zero, while the boundary condition (2.3) must also hold, we have immediately that

$$I(\Lambda_2) = 0 \quad . \tag{5.4}$$

The line integral about the outer circular boundary can be written in the form

$$I(\Lambda_1) = \frac{1}{2} r_0 \int_{-\pi}^{\pi} ([t_{xx}u_x + t_{xy}u_y]_{r_0} \cos\theta + [t_{yy}u_y + t_{xy}u_x]_{r_0} \sin\theta) d\theta \quad . \tag{5.5}$$

The elastic strain energy of the infinite plane body can therefore be expressed as the limit

$$U(\infty) = \lim_{r_0 \to \infty} I(\Lambda_1) + I(\Lambda_2) = \lim_{r_0 \to \infty} I(\Lambda_1) \quad . \tag{5.6}$$

Substitution of the series representations Eqs. (3.2) and (3.3) for the stress and displacements into line integral (5.5) leads to the following expression

$$I(\Lambda_1) = \frac{1}{2} \frac{\sigma^2}{16\mu} \int_{-\pi}^{\pi} [r_0^2 F(\theta;k,\alpha,\kappa) + a^2 G(\theta;\alpha,\kappa) + a^2 \sum_{n=1}^{\infty} \left(\frac{a}{r_0}\right)^{2n} H_n(\theta;k,\alpha,\kappa)] d\theta \quad , \tag{5.7}$$

where

$$
\begin{aligned}
F(\theta;k,\alpha,\kappa) &= A_1[A_4\cos^2\theta + A_5(\cos^2\theta\cos2\alpha + \sin\theta\cos\theta\sin2\alpha)] \\
&+ A_2[A_4\sin^2\theta + A_5(\sin\theta\cos\theta\sin2\alpha - \sin^2\theta\cos2\alpha)] \\
&+ A_3[A_4\sin\theta\cos\theta + A_5(\cos^2\theta\sin2\alpha - \sin\theta\cos\theta\cos2\alpha)] \\
&+ A_3[A_4\sin\theta\cos\theta + A_5(\cos\theta\sin\theta\cos2\alpha + \sin^2\theta\sin2\alpha)] \quad ,
\end{aligned} \tag{5.8}
$$

$$
\begin{aligned}
G(\vartheta;k,\alpha,\kappa) &= A_1(A_2[A_7\cos^2\theta + \sin\theta\cos\theta\sin2\theta] + A_3[A_6\sin\theta\cos\theta + \sin\theta\cos\theta\cos2\theta]) \\
&+ A_2(A_2[A_6\sin^2\theta - \sin^2\theta\cos2\theta] - A_3[A_7\sin\theta\cos\theta - \sin^2\theta\sin2\theta]) \\
&+ A_3(A_2[A_6\sin\theta\cos\theta - \sin\theta\cos\theta\cos2\theta] - A_3[A_7\cos^2\theta - \sin\theta\cos\theta\sin2\theta]) \\
&+ A_3(A_2[A_7\sin\theta\cos\theta + \sin^2\theta\sin2\theta] + A_3[A_6\sin^2\theta + \sin^2\theta\cos2\theta]) \\
&+ \tfrac{1}{2}[A_4\cos\theta + A_5(\cos\theta\cos2\alpha + \sin\theta\sin2\alpha)](A_2[\cos\theta\cos2\theta - 2\sin\theta\cos\theta\sin3\theta] \\
&\qquad - A_3[2\cos\theta\sin2\theta + 2\sin\theta\cos\theta\cos3\theta]) \\
&+ \tfrac{1}{2}[A_4\sin\theta + A_5(\cos\theta\sin2\alpha - \sin\theta\cos2\alpha)](A_2[\sin\theta\cos2\theta + 2\sin^2\theta\sin3\theta] \\
&\qquad + A_3[2\sin^2\theta\cos3\theta]) \\
&+ \tfrac{1}{2}[A_4\sin\theta + A_5(\cos\theta\sin2\alpha - \sin\theta\cos2\alpha)](A_2[2\sin\theta\cos\theta\cos3\theta] \\
&\qquad - A_3[2\sin\theta\cos\theta\sin3\theta - \cos\theta\cos2\theta]) \\
&+ \tfrac{1}{2}[A_4\cos\theta + A_5(\cos\theta\cos2\alpha + \sin\theta\sin2\alpha)](A_2[2\sin^2\theta\cos3\theta] \\
&\qquad - A_3[2\sin^2\vartheta\sin3\theta - \sin\theta\cos2\theta]) \quad ,
\end{aligned} \tag{5.9}
$$

and

$$
\begin{aligned}
A_1 &= (1+k)+(1-k)\cos2\alpha \quad , \quad A_2 = (1+k)-(1-k)\cos2\alpha \\
A_3 &= (1-k)\sin2\alpha \quad , \quad A_4 = (\kappa-1)(1+k) \\
A_5 &= 2(1-k) \quad , \quad A_6 = \tfrac{1}{2}(1+\kappa) \\
A_7 &= \tfrac{1}{2}(1-\kappa) \quad .
\end{aligned} \tag{5.10}
$$

The functions $H_n(\theta;k,\alpha,\kappa)$ appearing in the integrand of (5.7) are composed of sums and products of sine and cosine functions and have bound values over the interval $[-\pi,\pi]$. Thus for any n and all values of θ in the interval it is always possible to find numbers M and N such that the functions H_n satisfy the inequality $|H_1(\theta;k,\alpha,\kappa) + ... + H_n(\theta;k,\alpha,\kappa)| < M$ for any $n > N$. Futhermore, the sequence of positive coefficients $\left\{(a/r_0)^{2n}\right\}$ approach zero monotonically as $n \to \infty$. Under these circumstances it follows from the Dirichlet test for convergence [14] that the infinite series appearing in the integrand of Eq. (5.7) converges uniformly over $[-\pi,\pi]$. The order of integration with summation may therefore be interchanged, allowing expression (5.7), upon integration of the first two terms, to be reduced to

$$I(\Lambda_1) = \frac{\sigma^2\pi r_0^2}{16\mu}\,[k^2(1+\kappa)+2k(\kappa-3)+\kappa+1]$$

$$+ \frac{\sigma^2\pi a^2}{16\mu}\,[k^2+2k(2-\kappa)+1-(1-k^2)\cos 2\alpha] \qquad (5.11)$$

$$+ \frac{\sigma^2 a^2}{32\mu} \sum_{n=1}^{\infty} \left(\frac{a}{r_0}\right)^{2n} \int_{-\pi}^{\pi} H_n(\theta;k,\alpha,\kappa)\,d\theta \quad .$$

The infinite series of integrals converges to zero in the limit as $r_0 \to \infty$, that is,

$$\lim_{r_0\to\infty} \sum_{n=1}^{\infty} \left(\frac{a}{r_0}\right)^{2n} \int_{-\pi}^{\pi} H_n(\theta;k,\alpha,\kappa)\,d\theta = \lim_{r_0\to\infty} \left\{ \left(\frac{a}{r_0}\right)^2 H_1^*(k,\alpha,\kappa) + \left(\frac{a}{r_0}\right)^4 H_2^*(k,\alpha,\kappa) \right.$$

$$\left. + ... \right\} = 0 \quad , \qquad (5.12)$$

since $(a/r_0) < 1$, and $H_n^*(k,\alpha,\kappa)$ are finite numbers, the result of integration of the bound functions $H_n(\theta;k,\alpha,\kappa)$ on the interval $[-\pi,\pi]$.

It follows from Eqs. (5.6), (5.11) and (5.12), that the elastic strain energy of an infinite plane body which has an inclined central crack and which is load biaxially along its remote outer boundaries, can be expressed as the sum

$$U(\infty) = \lim_{r_0 \to \infty} I(\Lambda_1) = U_0 + \Delta U \quad , \tag{5.13}$$

where

$$U_0 = \lim_{r_0 \to \infty} \left[r_0^2 \frac{\sigma^2 \pi (1+\nu)}{8E} \left\{ k^2(1+\kappa)+2k(\kappa-3)+\kappa+1 \right\} \right] \tag{5.14}$$

represents the unbound elastic strain energy of the infinite body not having a crack, and

$$\Delta U = \frac{\sigma^2 \pi (1+\nu) a^2}{8E} [k^2+2k(2-\kappa)+1-(1-k^2)\cos 2\alpha] \tag{5.15}$$

is the change of the elastic strain energy associated with insertion of a crack of length 2a inclined at an angle α relative to direction of the tensile loading σ.

When the crack is horizontally oriented, $\alpha = \pi/2$, Eq. (5.15) reduces to the previously obtained form [3]

$$\Delta U_{\left(\alpha = \frac{\pi}{2}\right)} = \frac{\sigma^2 \pi (1+\nu) a^2}{4E} [1+k(2-\kappa)] \quad . \tag{5.16}$$

For the crack with a vertical orientation, $\alpha = 0$, and biaxial loading, the form for ΔU should be identical to Eq. (5.16) because of the symmetry of the two situations. Thus for $\alpha = 0$, letting $(\pm k)\sigma \equiv \tau$ so that $\sigma = \tau/(\pm k) = (\pm k')\tau$, substitution in Eq. (5.15) recovers the form given by Eq. (5.16), e.g., for $k > 0$,

$$\Delta U_{(\alpha = 0)} = \frac{\left(\frac{\tau}{k}\right)^2 \pi(1+\nu)a^2}{8E} [2k^2 + 2k(2-\kappa)]$$

$$= \frac{\tau^2 \pi(1+\nu)a^2}{4E} [1 + k'(2-\kappa)] \quad , \tag{5.17}$$

where τ is now the tensile load in the direction perpendicular to the plane of the crack and $k'\tau$ is the load parallel to the crack.

It is apparent from Eq. (5.15) that the elastic energy change ΔU can have the value zero when the horizontal load, the crack orientation and the Poisson ratio are such that the condition

$$k^2 + 2k(2-\kappa) + 1 - (1-k^2)\cos 2\alpha = 0 \tag{5.18}$$

is satisfied. There are several combinations of values of the parameters k, α, and ν, that will satisfy this condition. Among the more obvious are

$$\Delta U = 0 : \begin{cases} \alpha = \frac{\pi}{2} \quad , \quad k = \frac{1}{\kappa - 2} \\ \alpha = 0 \quad , \quad k = 0 \end{cases} \tag{5.19}$$

For the first case the crack is horizontal and the horizontal load parameter has values that depend on the Poisson ratio of the material, as shown in Table 1.

TABLE 1. Values of Load Biaxiality and Poisson's Ratio for Which $\Delta U = 0$ When the Crack is Horizontal ($\alpha = \pi/2$).

Plane Stress		Plane Strain	
Poisson Ratio ν	Load Biaxiality k	Poisson Ratio ν	Load Biaxiality k
0.25	5.00	0.25	*
0.30	13.00	0.30	-5.00
0.33	*	0.35	-2.50
0.40	-7.00	0.40	-1.67
0.45	-4.14	0.45	-1.25

*For no finite values of k.

When the Poisson's ratio has the particular values $\nu = 0.33$ for plane stress, and $\nu = 0.25$ for plane strain, the elastic strain energy change ΔU associated with insertion of the crack cannot have the value zero, regardless of the value of the load biaxiality k.

For the latter case, $\Delta U = 0$ when $k = 0$ and $\alpha = 0$, that is, when the applied load is uniaxial tension σ and the crack is oriented parallel to the direction of this tensile load. If we look upon this as the limit situation

$$\lim_{\substack{\alpha \to 0 \\ k \to 0}} (\Delta U) = 0 \quad , \tag{5.20}$$

then for small values of α and k, representing crack inclinations close to the vertical direction and horizontal loads of small magnitudes, the values for ΔU will be correspondingly small.

For any of the circumstances for which the parameters k, α, ν are collectively such as to satisfy Eq. (5.18), insertion of the crack (or, mathematically speaking, a slit) into the biaxially loaded plane body will not cause any change of the total elastic strain energy of that body. Hence, as U_0 in Eq. (5.13) is independent of the crack dimension, $dU/da = d(U_0 + \Delta U)da = 0$ in Eq. (4.7), causing the Griffith fracture criterion, as expressed by this form, to become inapplicable.

6. The Critical or Fracture Load

The critical tensile load, σ_c, is obtained by application of the Griffith crack instability criterion (4.7), where $\Gamma = 4\gamma a$ is the crack surface energy, and expressions (5.13)-(5.15) represent the total elastic strain energy of the infinite body. Thus the condition for the stationary value of the potential energy of the system

$$\frac{d}{da}\left[\Gamma - U(\infty)\right] = \frac{d}{da}\left[4\gamma a - (U_0 + \Delta U)\right] = 0 \quad , \tag{6.1}$$

leads to the following expression for the critical tensile load for an inclined crack

$$\sigma_c = \left\{ \frac{16E\gamma}{\pi a(1+\nu)} \quad \frac{1}{[k^2+2k(2-\kappa)+1-(1-k^2)\cos 2\alpha]} \right\}^{1/2} \quad . \tag{6.2}$$

In addition to the crack size, the values of the elastic modulus and the crack surface energy density, the fracture load according to this criterion is also governed by three additional parameters, namely, the horizontal load (or load biaxiality), the crack orientation and the Poisson ratio of the material,

$$\sigma_c = f(a,\alpha,k,\nu,E,\gamma) \quad . \tag{6.3}$$

When the parameter values are such that Eq. (5.18) holds, σ_c as given by Eq. (6.2) appears to become unbounded in value. Actually this corresponds to the condition that $\Delta U = 0$, with corresponding inapplicability of the fracture criterion.

Figures 4 to 17 illustrate graphs of the expressions

$$\sigma_c\left(\frac{\pi a}{16E\gamma}\right)^{1/2} = \left\{\frac{1}{(1+\nu)\left[k^2+2k\left(\frac{3\nu-1}{1+\nu}\right)+1-(1-k^2)\cos 2\alpha\right]}\right\}^{1/2} \quad \text{(plane stress)} \quad (6.4)$$

and

$$\sigma_c\left(\frac{\pi a}{16E\gamma}\right)^{1/2} = \left\{\frac{1}{(1+\nu)\left[k^2+2k(4\nu-1)+1-(1-k^2)\cos 2\alpha\right]}\right\}^{1/2} \quad \text{(plane strain)} \ , \quad (6.5)$$

for different values of the load biaxiality, the crack orientation and the Poisson ratio of the material. Symmetry considerations with respect to the vertical tensile load direction reduce consideration of the crack orientations to the range $0° \leq \alpha \leq 90°$.

When the crack is horizontally oriented, $\alpha = \pi/2$, the fracture stress variation with load biaxiality is monotonic for all Poisson ratio values for both plane stress and plane strain, as shown by Figures 4 and 8. There is a qualitative change of the variation of σ_c with k as the Poisson ratio value varies from $\nu = 0.25$ to $\nu = 0.45$. For plane stress, σ_c increases as k increases in the tensile sense for values of $\nu < 0.33$, while it decreases as k increases in the tensile sense when $\nu > 0.33$. A similar pattern exists for plane strain, except that the dividing value for the Poisson ratio is now $\nu = 0.25$. Referring to Table 1, for $\nu = 0.33$ and plane stress, or $\nu = 0.25$ and plane starin, the elastic strain energy associated with insertion of the crack, ΔU, will have a non-zero value for all values of k. This is also shown in Figures 4 and 8. Table 1 also lists the collective sets of values of k and ν at which $\Delta U = 0$. For these sets of values the denominator of Eq. (6.2) has the value zero, giving the apparency of $\sigma_c \to \infty$. This is illustrated, for example, in Fig. 8 for $\nu = 0.45$ with the load biaxiality approaching the value $k = -1.25$.

As the crack inclination angle is decreased toward the vertical orientation, the curves of Figures 5-7, 9-11 and 12-17 show a peak effect developing in the vicinity of uniaxial loading, k = 0, becoming increasingly pronounced as the crack angle gets smaller and approaches a direction parallel to the tensile load σ. When the applied load is uniaxial tension and the crack angle is parallel to the load direction, the limit condition (5.20) holds and, correspondingly, the fracture load $\sigma_c \to \infty$, implying that it is not possible to cause fracture under these circumstances. It follows, therefore, that for crack orientations that are close to being vertical and with load biaxiality small, giving a loading condition that is almost uniaxial tension, the quantity ΔU will be small. Correspondingly the value for the fracture stress, σ_c, becomes comparatively large [cf. Eqs. (5.15) and (6.2)]. This peak effect appears to be in accord with the expectation that it becomes more difficult to effect fracture (i.e., larger values for σ_c) when the crack is aligned almost parallel to the tensile vertical load direction while the horizontal load is zero, or close to zero. According to Fig. 17, this effect is most pronounced for a material with a high Poisson ratio value in a condition of plane strain.

Figures 12-17 illustrate that at the particular load biaxiality of equal tension-tension, i.e., k = 1.0, the orientation of the crack is immaterial to the value of the critical tensile load. This is the case for all values of the Poisson ratio for both plane stress and plane strain.

The difference in values of the fracture stress between plane stress and plane strain conditions (sheet thickness) are greatest for the horizontal crack orientation as the load biaxiality intensifies in tension for plane stress and in compression for plane strain.

For each crack orientation, for both plane stress and plane strain, there is a corresponding horizontal compressive load, ranging between $-0.5 \leq k < 0$, at which the fracture stress has the same value for all values of the Poisson ratio, as shown in Figs. 4-11. To the left of this cross-over point σ_c increases as the value of ν increases, whereas to the right of this point σ_c decreases as the value of ν increases.

7. Fracture Stress Test Data For the Horizontally Oriented Crack

Ever since Griffith's first tests measuring the breaking stress of cracked glass tubes in 1921, there have been only a few other fracture test programs in which the loads have been applied biaxially [6-9]. Moreover, in all of these tests the crack orientations were parallel to the horizontally applied load, i.e., $\alpha = \pi/2$. The fracture load test data obtained from these tests, although previously reported, are collected and reproduced here because they provide some measure against which to judge qualitatively the results of the analysis, as indicated by Figures 4 and 8 for the horizontal crack orientation. The tests were performed on glass, several aluminum alloys and several plastics.

Glass [9]

The test specimens consisted of cylindrical glass tubes having a 0.02 in. wall thickness, and inner diameters that ranged from 0.59 in. to 0.74 in. The tubes were cracked along the axial direction, annealed and broken by internal pressure and end loading. The values of the elastic modulus, Poisson ratio and surface energy density for the glass were measured (directly and indirectly) to be: $E = 9.01 \times 10^6$ psi, $\nu = 0.25$, $\gamma = 3.1 \times 10^{-3}$ psi. The load biaxiality that was attained in these tests ranged only from $k = -0.9$ to $k = 0.5$.

Along side of the test results shown in Fig. 18 are Griffith's 1921 calculation of the critical stress

$$\sigma_c \sqrt{a} = \left(\frac{2E\gamma}{\pi} \right)^{1/2} \qquad \text{(1921)} \quad , \qquad (7.1)$$

and his subsequently revised calculation (for plane stress)

$$\sigma_c\sqrt{a} = \left(\frac{2E\gamma}{\pi}\right)^{1/2} \qquad (1924) \quad . \qquad (7.2)$$

In both calculations σ_c is independent of the load biaxiality, and in the second calculation it is also independent of the Poisson ratio of the material.* Also shown is a plot of Eq. (6.2) over the test range of the load biaxiality, which for $\alpha = \pi/2$ and plane stress becomes

$$\sigma_c\sqrt{a} = \left\{\frac{8E\gamma}{\pi}\left[\frac{1}{k(3\nu-1)+1+}\right]\right\}^{1/2} \quad . \qquad (7.3)$$

In the absence of any reason to think otherwise, it would be easy to interpret this test data as indicating a null effect for the load biaxiality on the critical stress, in agreement with Griffith's calculations, qualitatively at least. While it would be difficult to draw any conclusions from the limited data shown in Fig. 18, it appears nevertheless that Eq. (7.3) comes closer to fitting this data than do either of the Griffith formulas.

Aluminum Alloys [6,7]

Plane stress fracture toughness tests from K_c under biaxial loading conducted on 7075-T6, 2024 T-3 and 6061-T4 aluminum alloys. Specially designed sheet speciemns were used in a loading rig that was designed to apply loading independently in two directions. The specimens were 0.063 in. in thickness and had crack length to width ration, (2a/W), ranging between 0.40 to 0.50. The Poisson ratio of these alloys is approximately 0.30. The critical tensile stress σ_c was calculated from the reported K_c

*A critical discussion of these calculations may be found in Ref. [3].

values by means of the expression

$$\sigma_c = \frac{K_c}{\sqrt{\pi a}\, f\left(\frac{2a}{W}\right)} \tag{7.4}$$

where

$$f\left(\frac{2a}{W}\right) = \left[1 - (0.1)\left(\frac{2a}{W}\right) + \left(\frac{2a}{W}\right)^2\right] = 1.20$$

is the finite width correction factor used in the test program.

7075-T6

The results of two test series for this alloy are shown by Figures 19 and 20, where the load biaxiality ranged from k = 0 to k = 1.8. Higher k values could not be tested successfully because the horizontal loading tabs of the sheet specimens were pulled off prior to unstable fracture, thus releasing the biaxial constraint. Both series show a steady increase of the fracture stress with increase in the magnitude of the horizontal tensile loading up to k = 1.5, dropping off somewhat at the limit horizontal constraint value for tab pull out at k = 1.8. Successful biaxial fracture testing at higher tensile constraint loading beyond the k = 1.8 limit would require the use of thicker sheet specimens. The difference in the sets of values shown by Figures 19 and 20 is attributed to the anisotropy induced by the processing of the material.

2024T-3

Figures 21 and 22 show the results of two test series for this alloy. For this more ductile alloy the load biaxiality was limited to the maximum value of k = 1.5 because of loss occasioned by horizontal tab pull out. Both series show an increase of the fracture stress as k increases k = 0.0

to 0.5. The fracture load then decreases to a value at k = 1.5 approximately equal to the value of σ_c at k = 0, i.e., at uniaxial tensile loading.

6061-T4

The one series of test results for this alloy is shown by Fig. 23. The maximum horizontal constraint that could be sustained successfully by this alloy at 0.063 in. sheet thickness was only k = 1.25. The pattern of variation of σ_c versus k is similar to that for 2024-T3, with a peak value for σ_c at k = 0.5, followed by a decrease to a level at k = 1.25 approximately equal to the value for σ_c at k = 0.

An explanation for the appearance of the peak values for σ_c at k = 0.5 load biaxiality for the 2024-T3 and 6061-T4 tests could not be given. Since horizontal tab failures (pull out) prior to fracture did occur at the higher k values, it was conjectured that possibly the horizontal tabs of the test specimens for the more ductile alloys began to yield prior to the onset of unstable fracture, thus causing partial loss of the horizontal constraint. However this could not be verified by direct experimental observation.

Plastics [6,7,8]

Three test series were conducted on polyvinylchloride, PVC, and polymethylmethacrylate, PMMA, (plexiglass). Two were run at The George Washington University using the same biaxial load set-up and specimen design as for the aluminum series, while the other was performed at the Imperial College of Technology, London. The test specimen thicknesses were 0.25 in. and 0.16 in. The Poisson ratio for these plastics range

approximately between 0.40-0.45. The 0.25 in. thickness specimens gave the appearance of plane strain fracture conditions.

PVC

The fracture test results for this plastic is shown by Fig. 24. The fracture stress decreases steadily as the load biaxiality is increased in tension from k = 0 to k = 1.5

PMMA

The two sets of test results for PMMA are shown by Figures 25 and 26. Both show a wide degree of scatter of the data. However the linear regression lines for both sets show σ_c to be decreasing over the range of load biaxiality from k = -0.50 to k = 2.75, with the regression lines almost parallel.

8. Conclusions

The test data that is available for horizontally oriented cracks shows rather convincingly that the critical tensile load is influenced by the presence of the horizontal load and, also, by the Poisson ratio of the material. Furthermore, the nature of the dependency is, qualitatively speaking, in agreement with the results of the critical load calculation illustrated by Figures 4 and 8.

It is apparent from the two term nature of the Griffith global fracture criterion, Eqs. (4.7) or (6.1), that the criterion loses its applicability for those circumstances in which the elastic strain energy of the entire body can remain unaltered as the crack is extended, i.e., $dU/da = 0$. It is not difficult to imagine a physcially plausible situation where this can take place.

Moreover, in application of the fracture criterion for determination of the fracture stress for an inclined crack in a biaxially loaded plane infinite body, calculation of the elastic strain energy of the body also reveals that there are conditions for the load biaxiality, crack orientation and material Poisson ratio at which the derivative of the total strain energy with respect to crack size can have the value zero. This would appear to indicate that the Griffith global fracture criteria is of limited generality, even for entirely elastic material behavior throughout the body.

ACKNOWLEDGMENT

This work was partially completed while the first author was at the Naval Research Laboratory as part of the 1985 ASEE-Navy Summer Faculty Research Program. The authors wish to thank Drs. Peter Matic and Robert Badaliance and Mr. Daniel Briller for their assistance, support and interest.

REFERENCES

[1] J.Eftis, N. Subramonian and H. Liebowitz, Crack Border Stress and Displacement Equations Revisited, Engr. Fracture Mechanics, V. 9, 189, (1977).

[2] J. Eftis and N. Subramonian, The Inclined Crack Under Biaxial Load, Engr. Fracture Mechanics, V. 10, 43, (1978).

[3] J. Eftis and D.L. Jones, Influence of Load Biaxiality on the Fracture of Center Cracked Sheets, Int. Journ. of Fracture, V. 20, 267, (1982).

[4] J. Eftis, Influence of Load Biaxiality on the Fracture Characteristics of Two Collinear Cracks, Int. Journ. of Fracture, V. 24, 59, (1984).

[5] J. Eftis and N. Subramonian, The Cracked Shear Panel, AIAA Journal, V. 18, No. 3, 324, (1980).

[6] D.L. Jones and J. Eftis, Fracture and Fatigue Characterization of Aircraft Structural Materials Under Biaxial Loading. Report No. TR-81-0856, 1981, AFOSR, Bolling Air Force Base, Washington, DC.

[7] D.L. Jones, P.K. Poulose and H. Liebowitz, The Effects of Biaxial Loading on the Fracture Characteristics of Several Engineering Materials, forthcoming in Engr. Fracture Mechanics.

[8] J.C. Radon and P.S. Leevers, Fracture Toughness of PMMA Under Biaxial Stress, in Fracture 1977, V. 3, 1113, ICF4, Waterloo, 1977.

[9] A.A. Griffith, The Phenomena of Rupture and Flow in Solids, Philosophical Trans., Royal Soc., London, V. 221, 163, (1921).

[10] N.I. Muskhelishvili, Some Basic Problems of the Mathematical Theory of Elasticity, Noordhoof, Groningen, 1963.

[11] A.A. Griffith, The Theory Rupture, Proc. 1st Int. Conf. Appl. Mechanics, 55, Delft, 1924.

[12] I.S. Sokolnikoff, Mathematical Theory of Elasticity, McGraw-Hill, New York, 1956.

[13] W. Kaplan, Advanced Calculus, Addison-Wesley, Reading, Mass., 1959.

[14] R.G. Bartle, The Elements of Real Analysis, J. Wiley, New York, 1964.

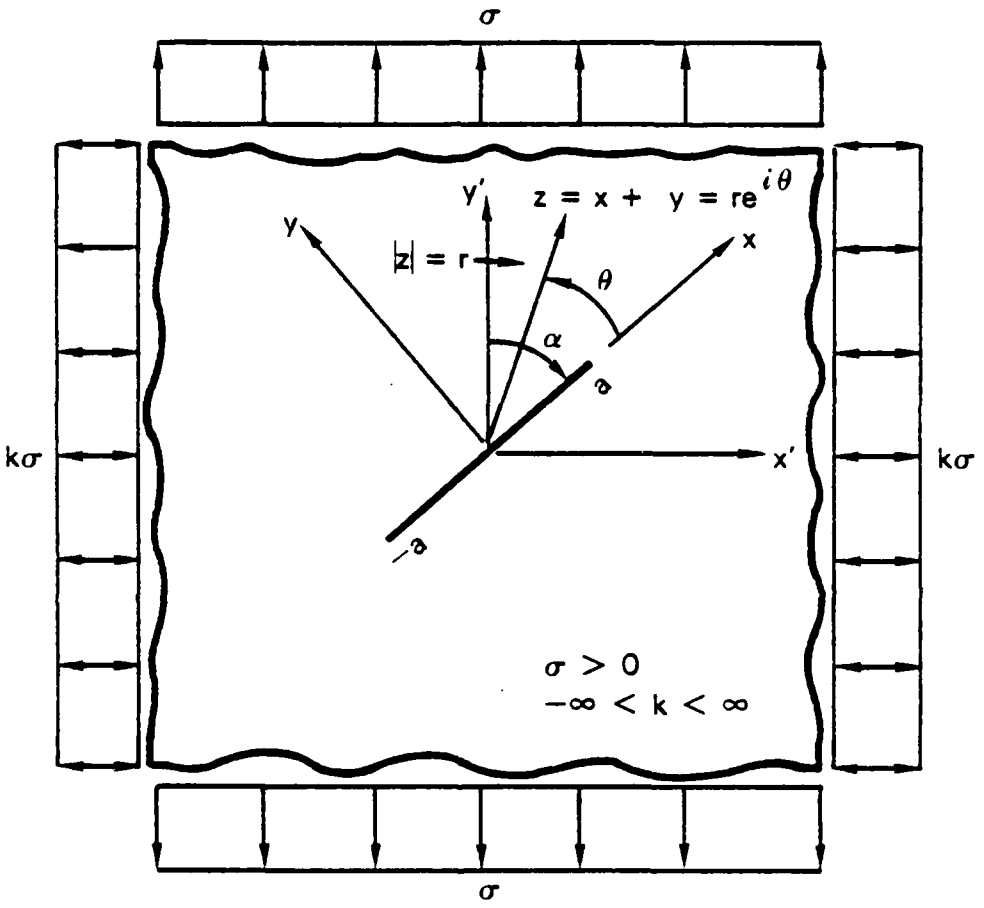

Fig. 1 — Crack geometry and boundary tractions.

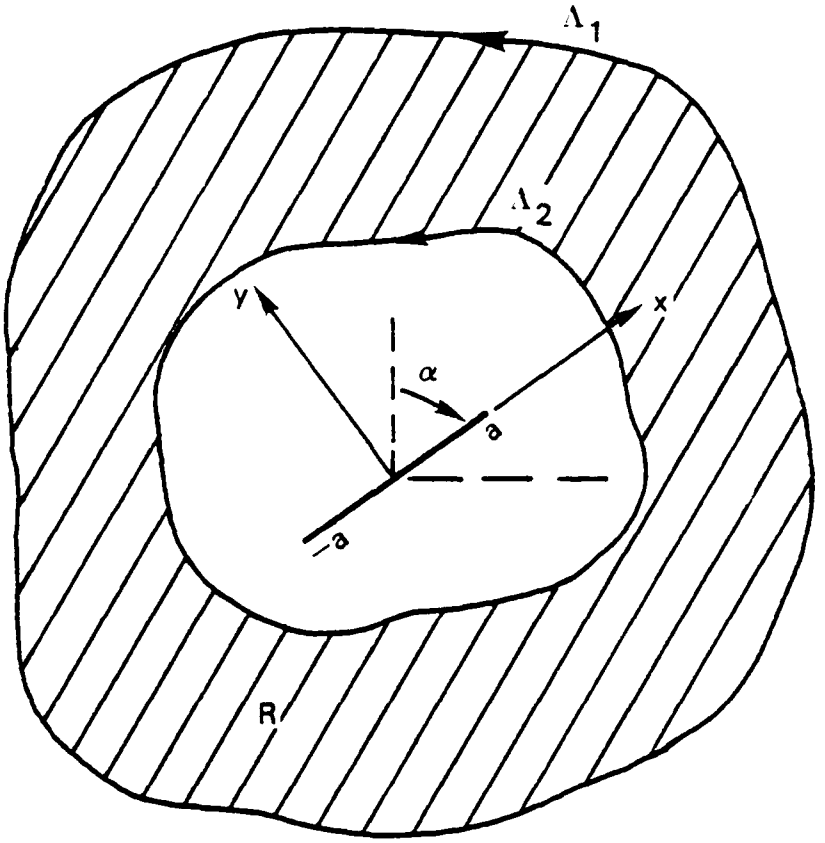

Fig. 2 — Bound plane region R enclosing the crack.

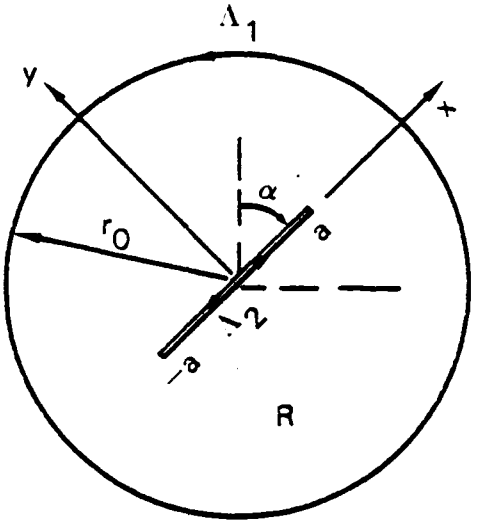

Fig. 3 — Region R bound by circular contour Λ_1 and crack contour Λ_2.

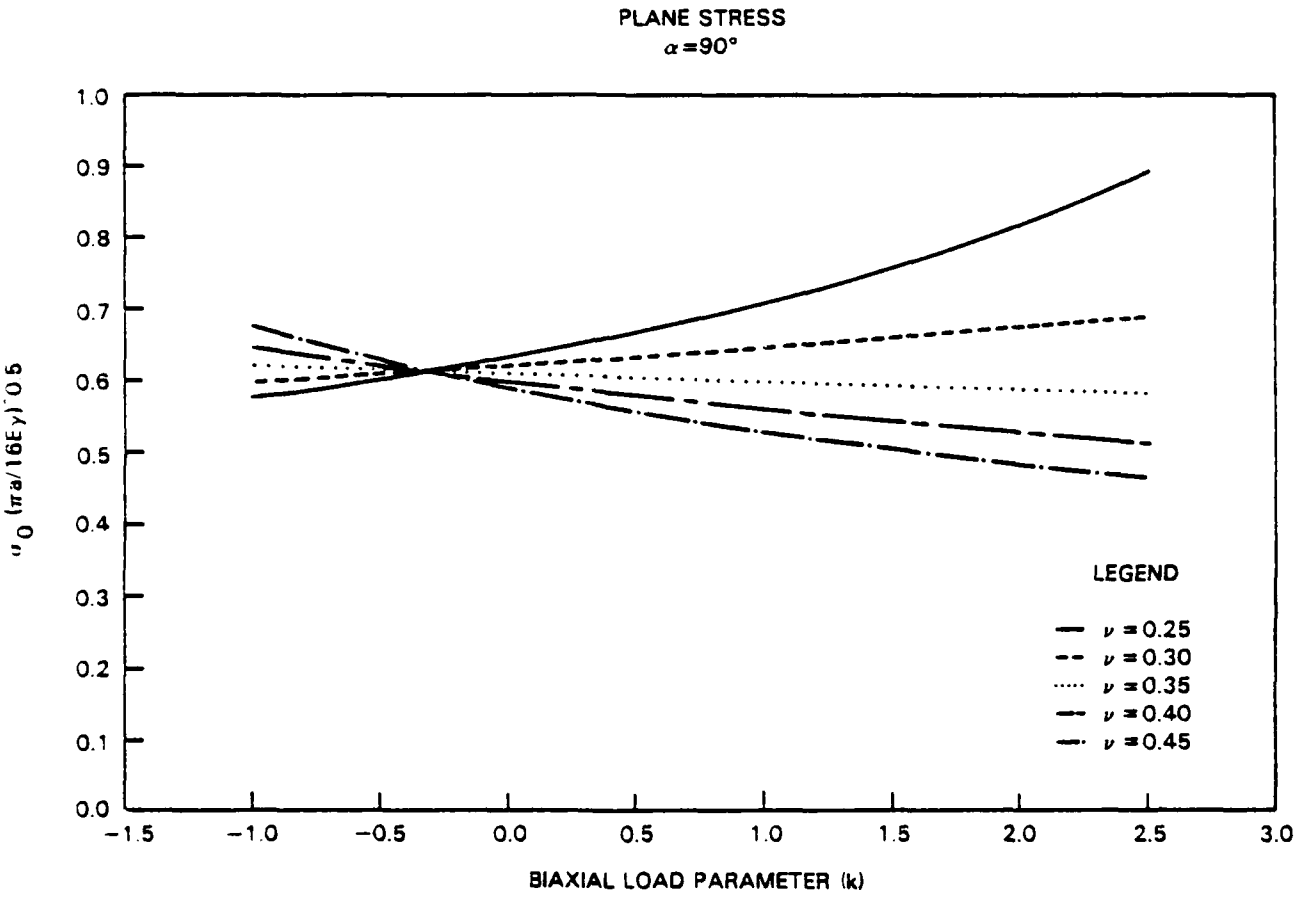

Fig. 4 — Fracture load versus load biaxiality.

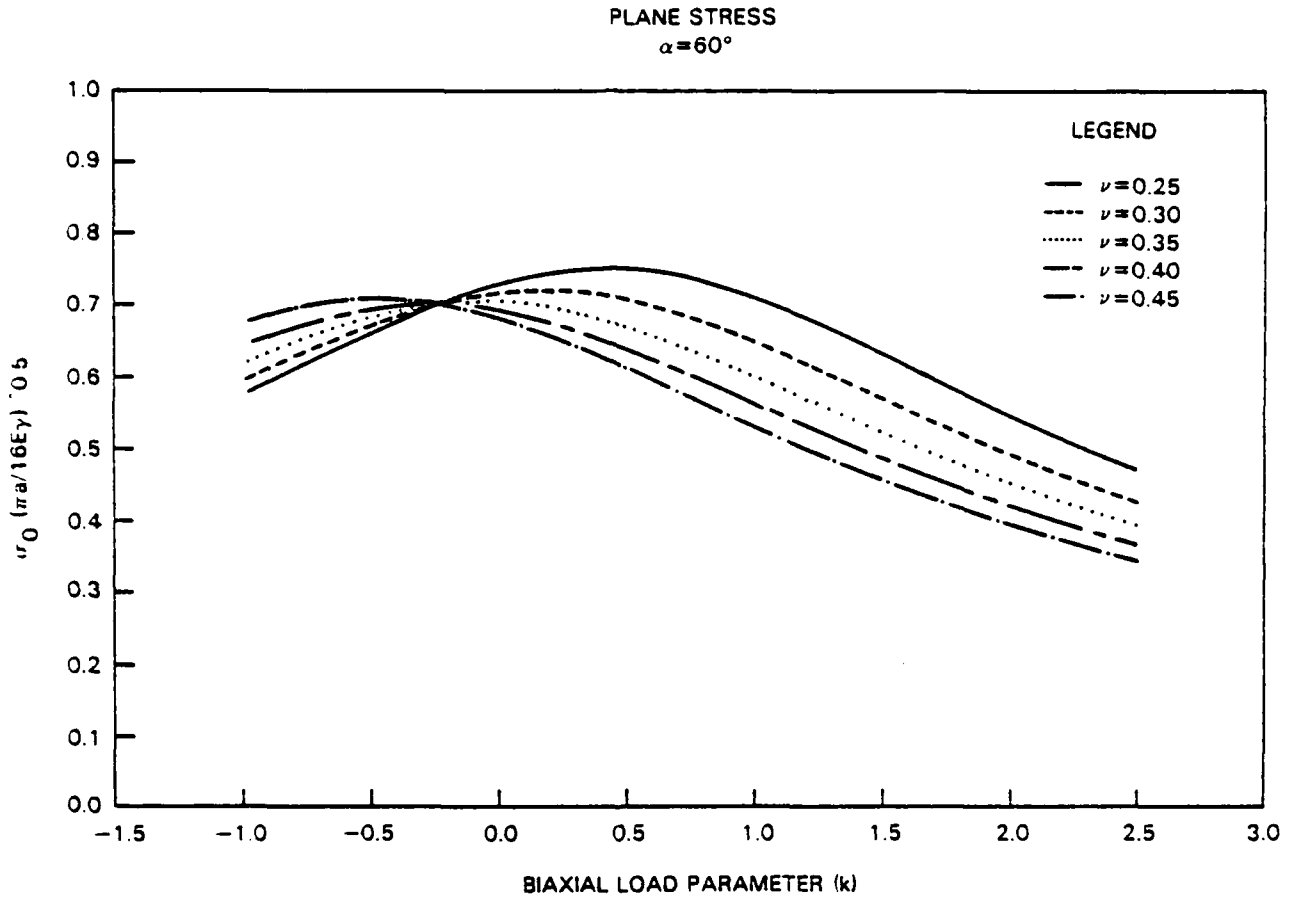

Fig. 5 — Fracture load versus load biaxiality.

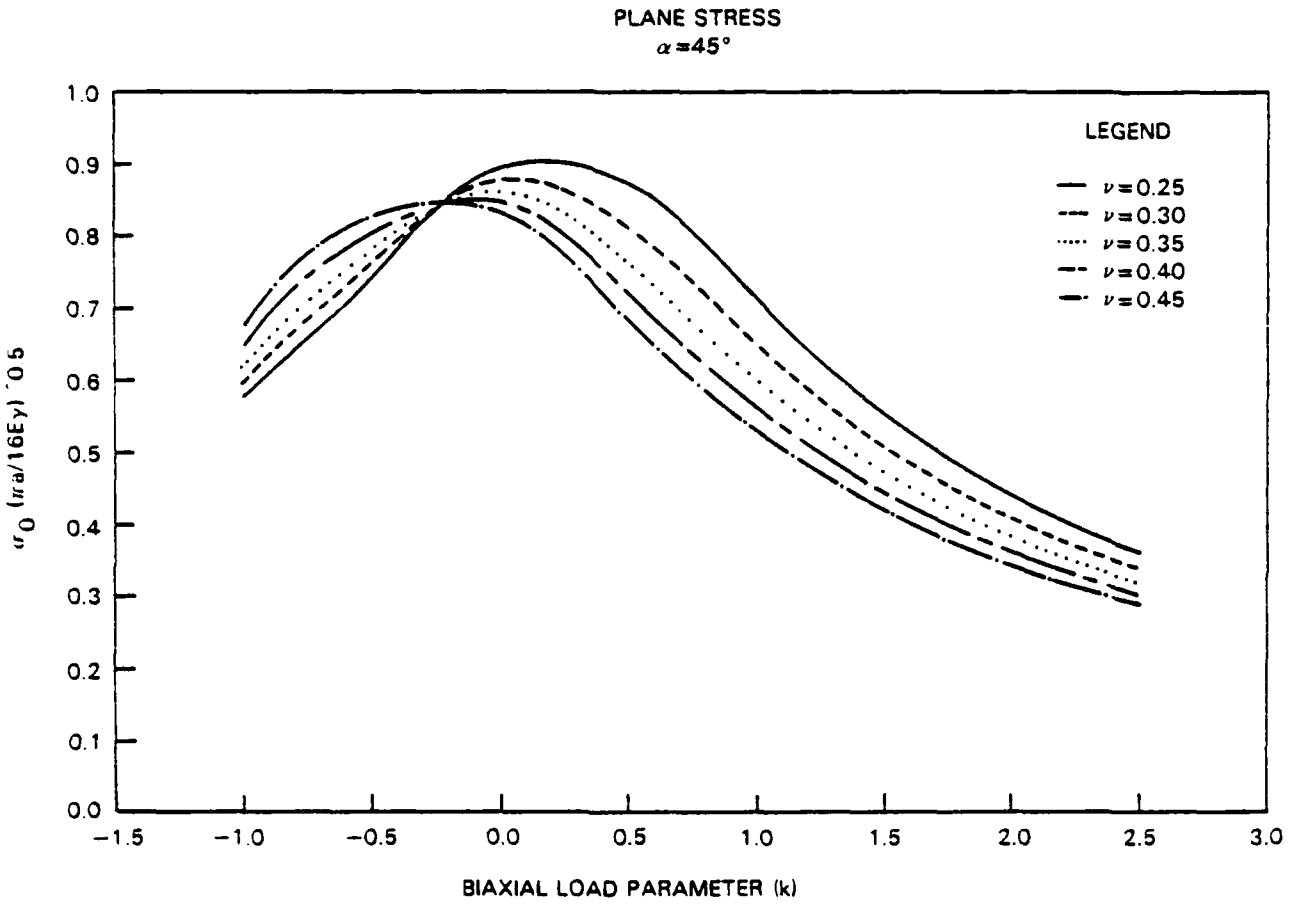

Fig. 6 — Fracture load versus load biaxiality.

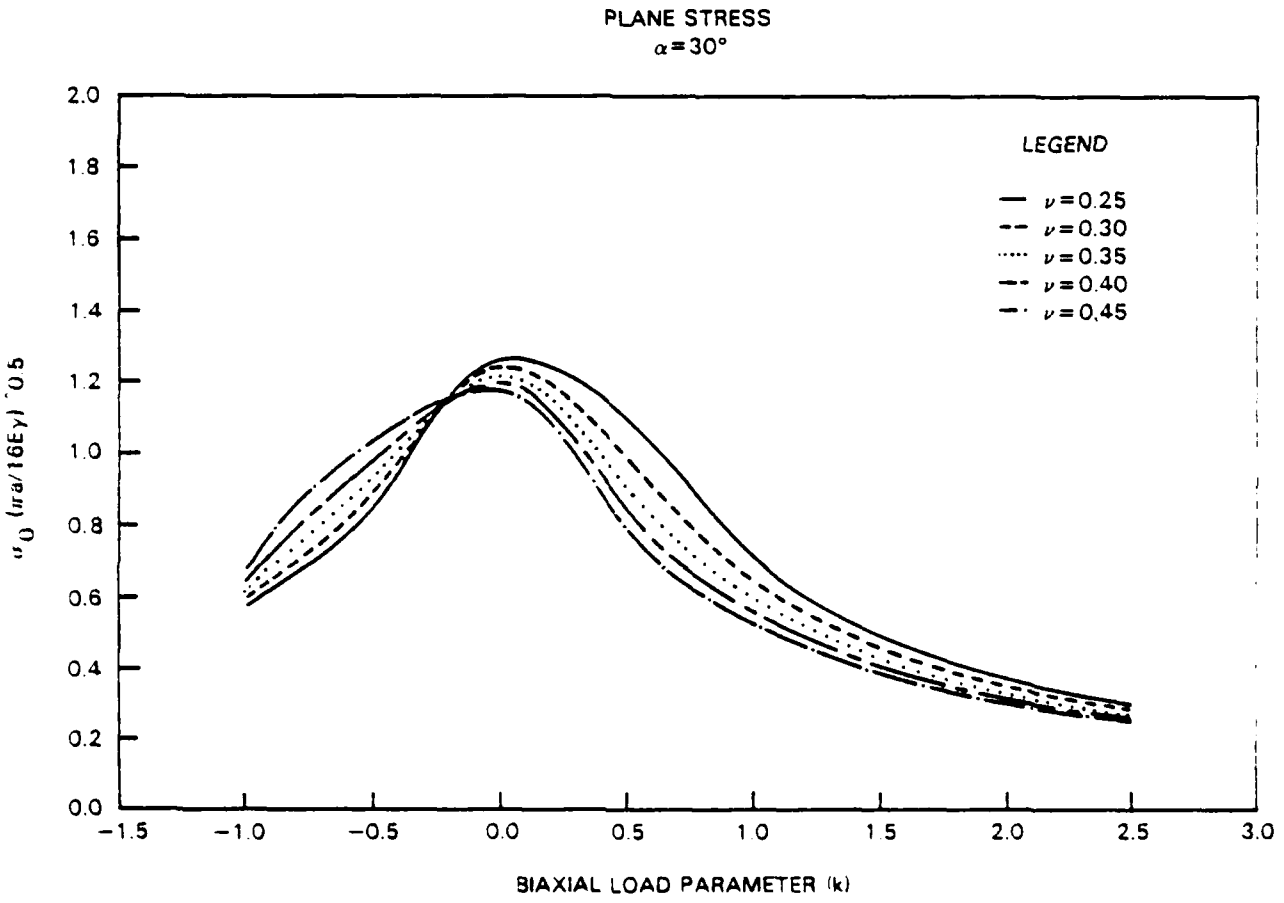

Fig. 7 — Fracture load versus load biaxiality.

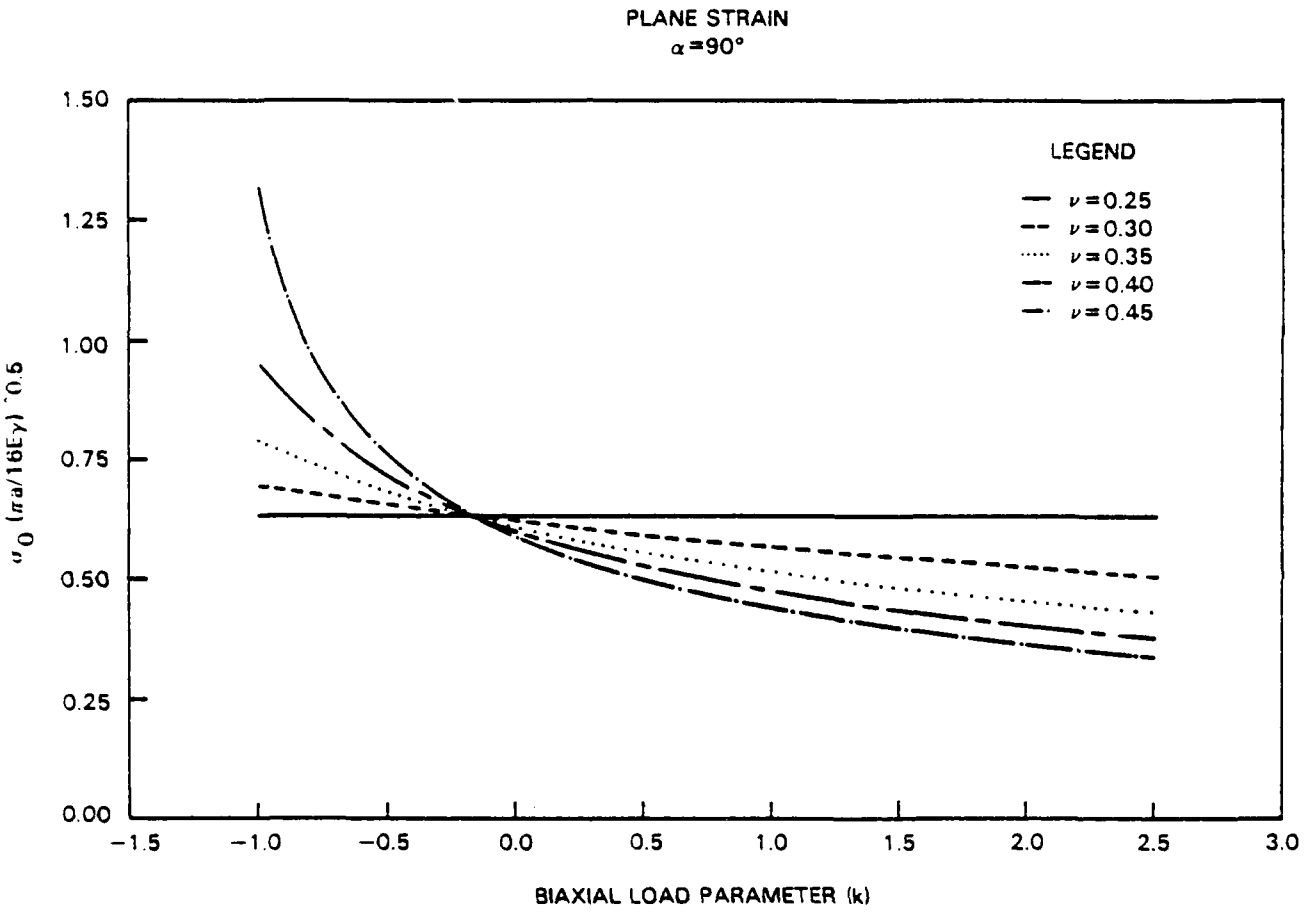

Fig. 8 — Fracture load versus load biaxiality.

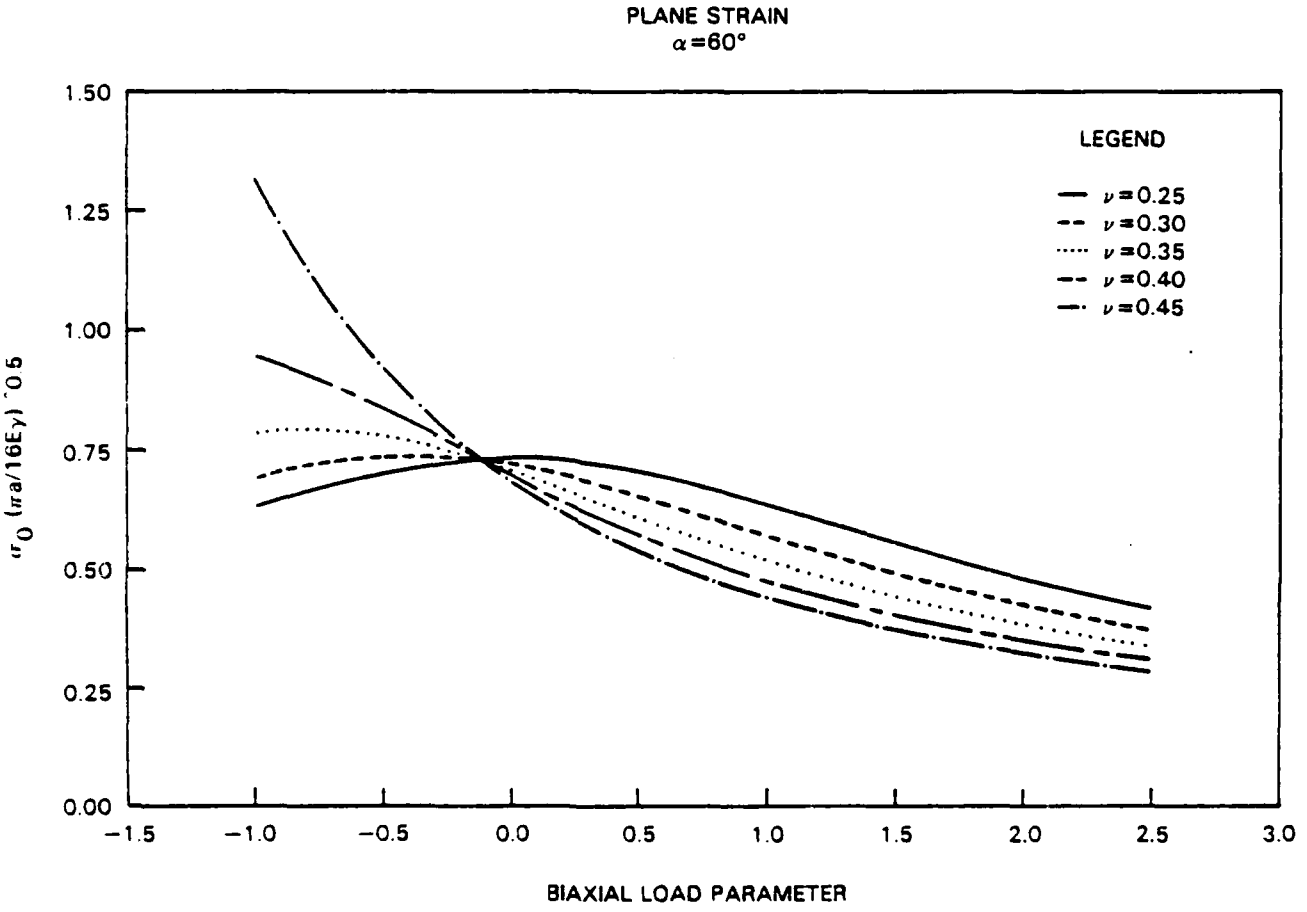

Fig. 9 — Fracture load versus load biaxiality.

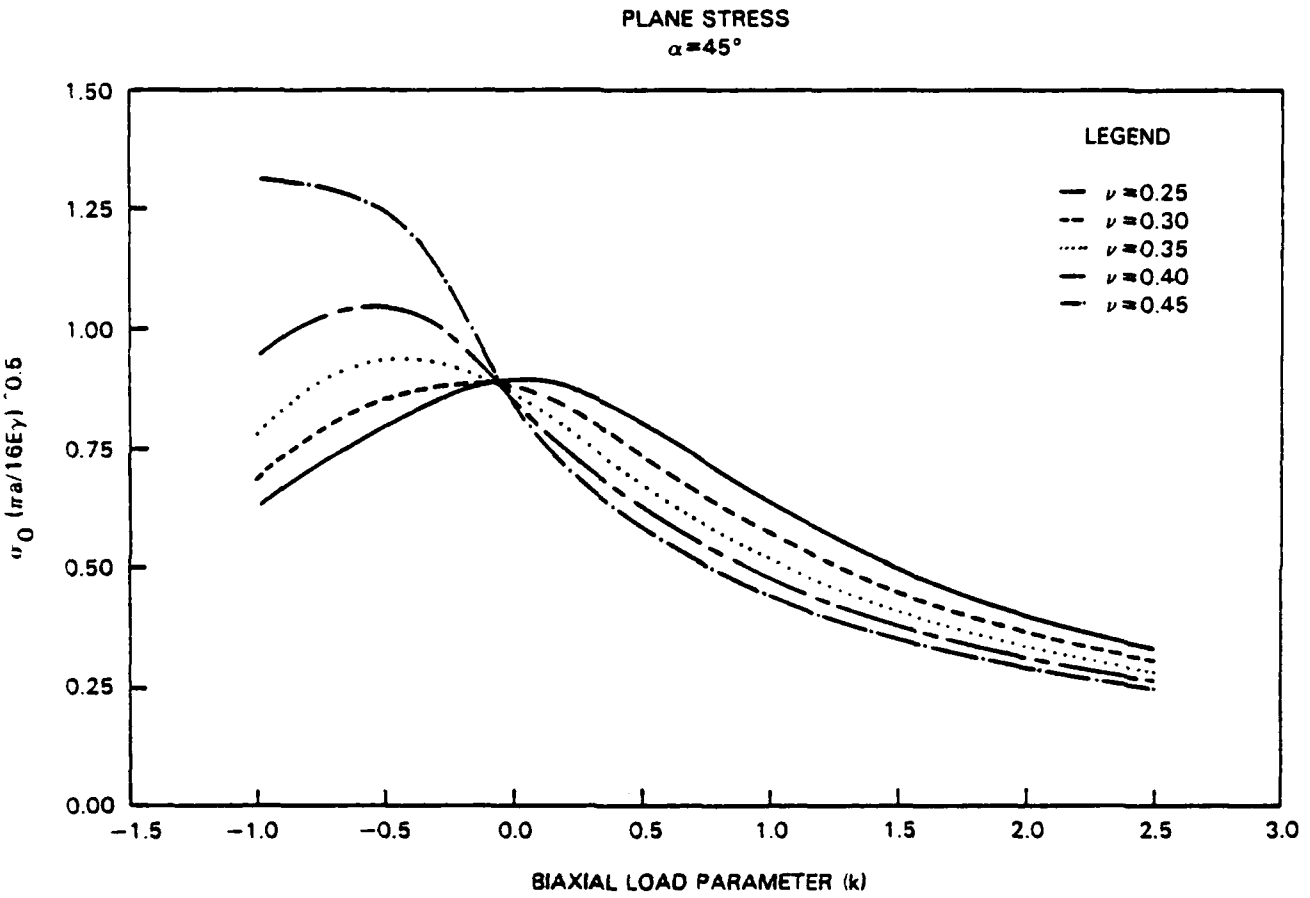

Fig. 10 — Fracture load versus load biaxiality.

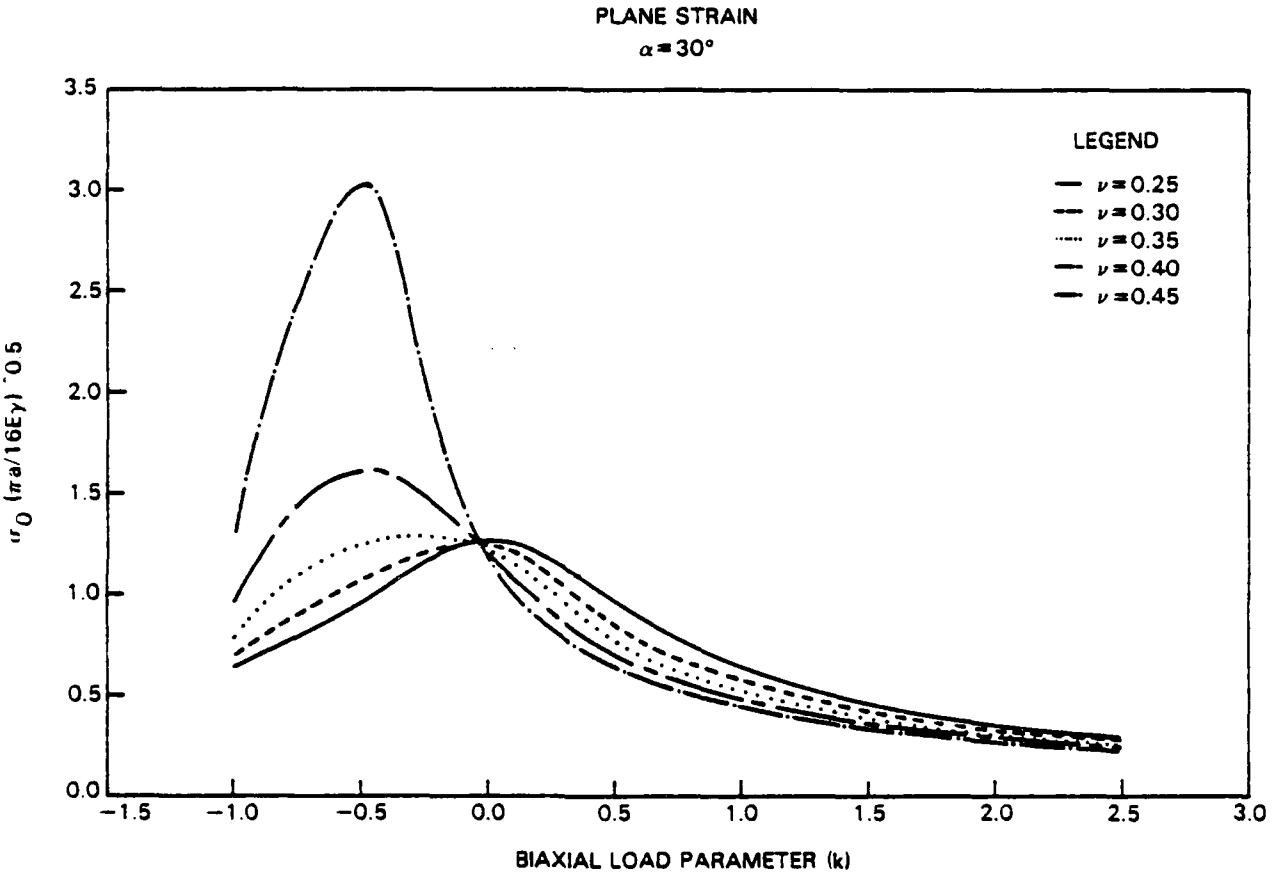

Fig. 11 — Fracture load versus load biaxiality.

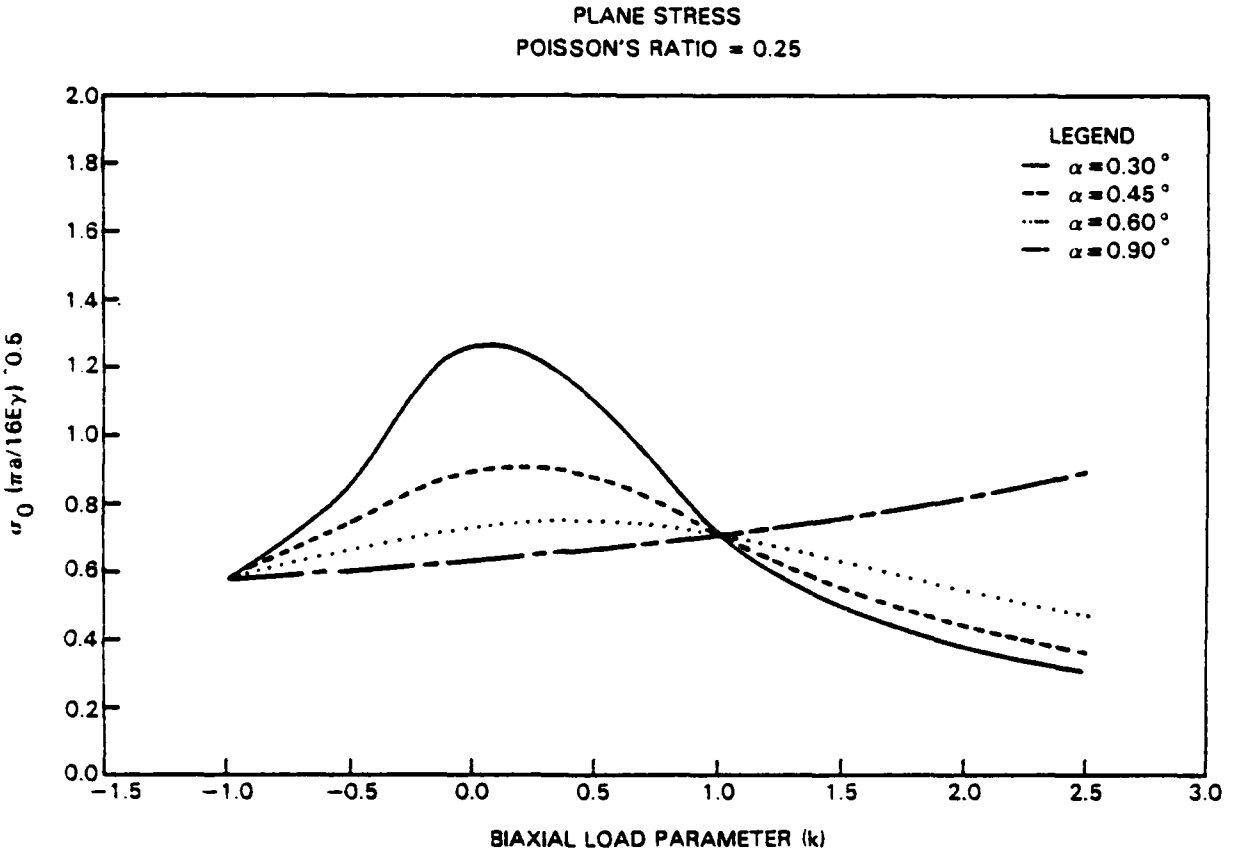

Fig. 12 — Fracture load versus load biaxiality.

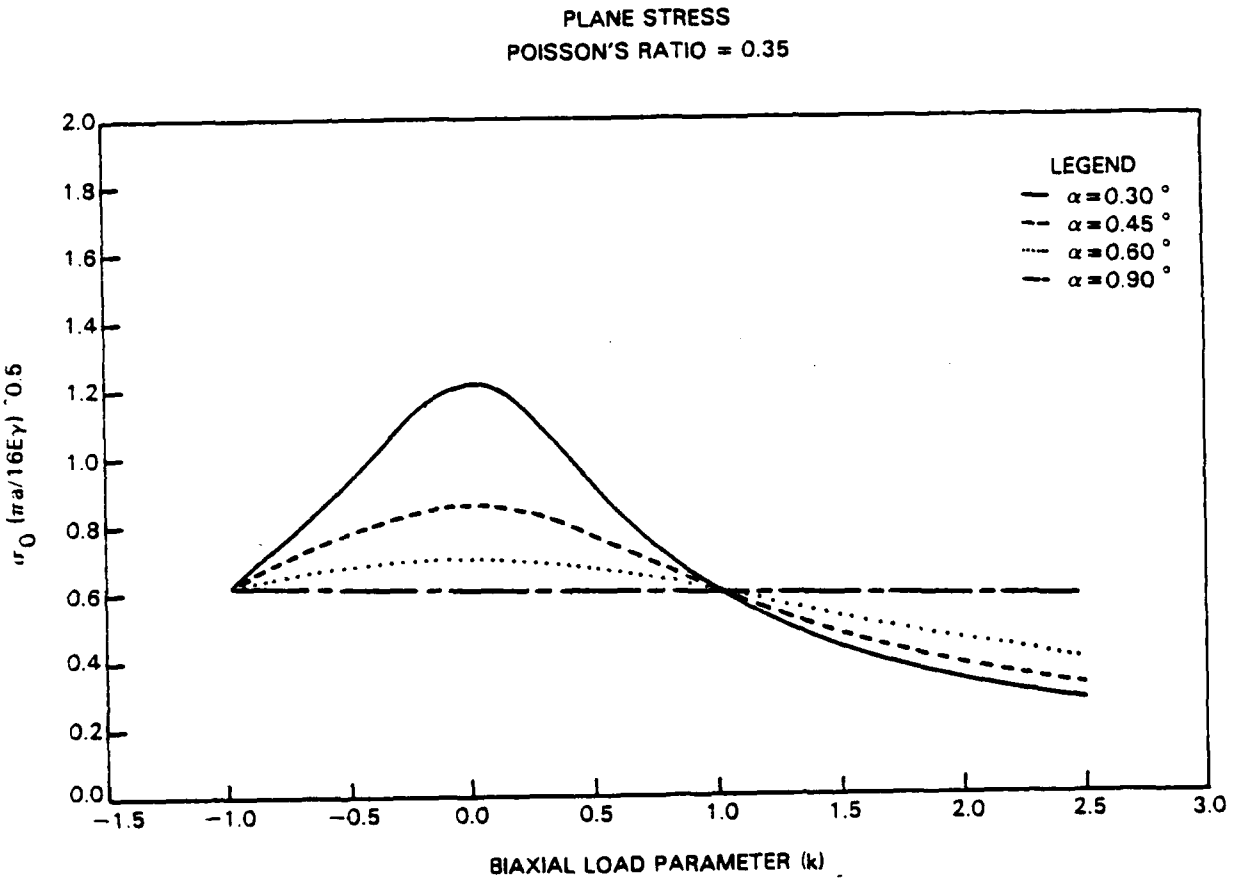

Fig. 13 — Fracture load versus load biaxiality.

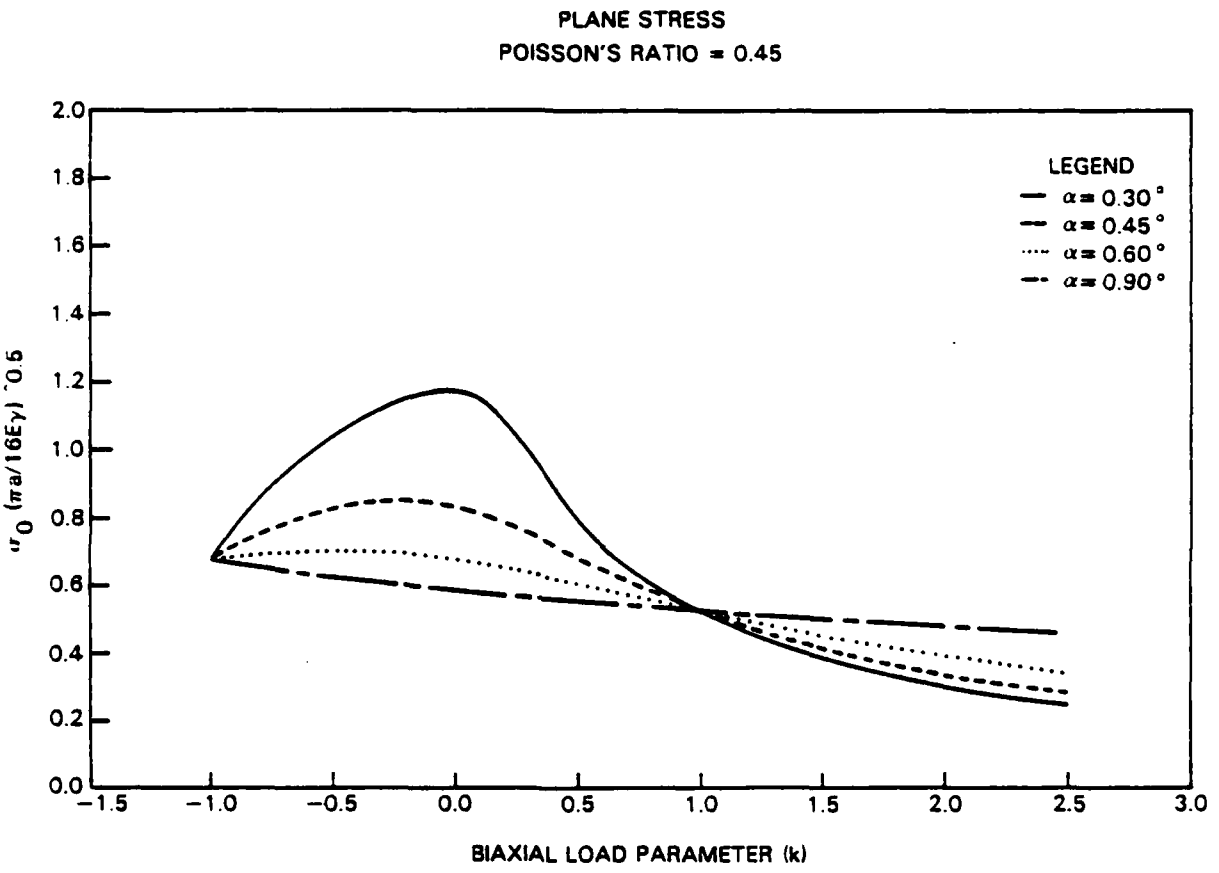

Fig. 14 — Fracture load versus load biaxiality.

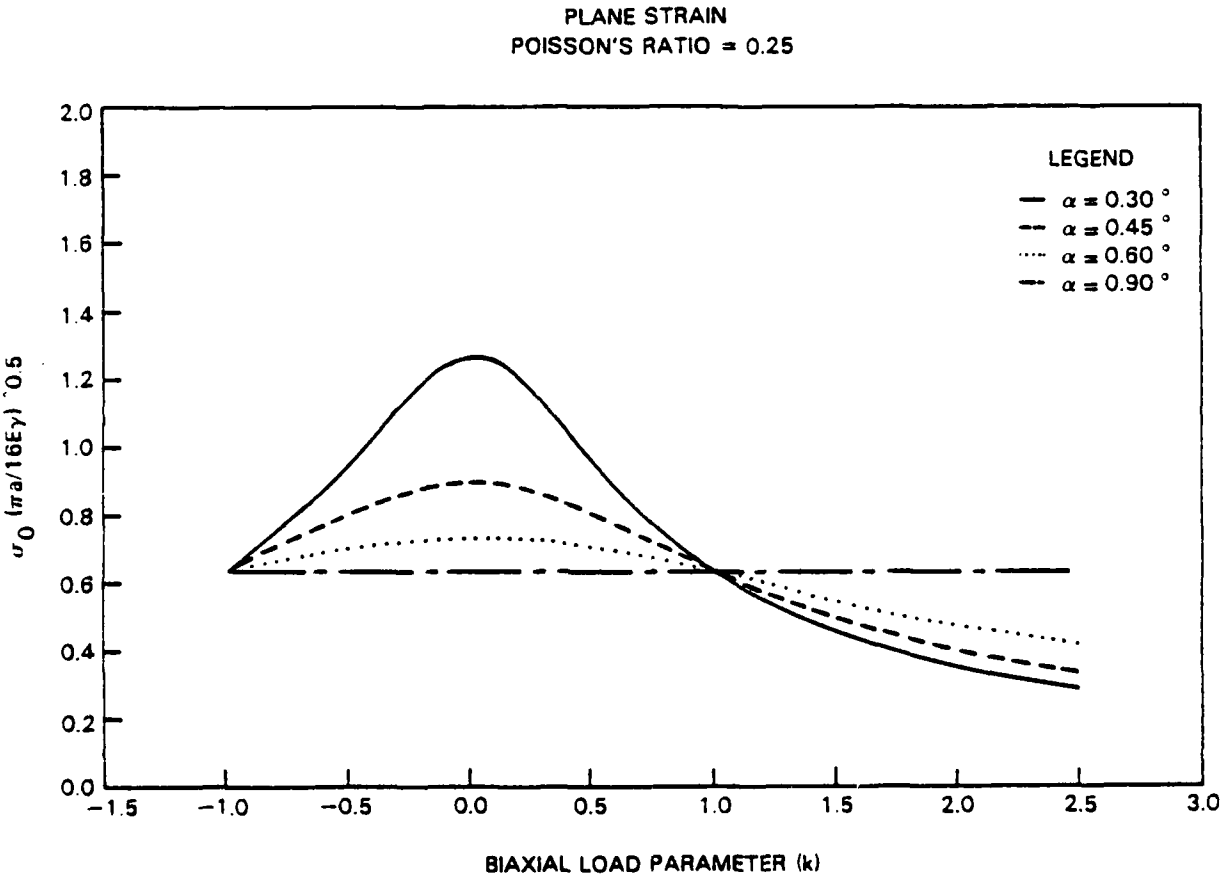

Fig. 15 — Fracture load versus load biaxiality.

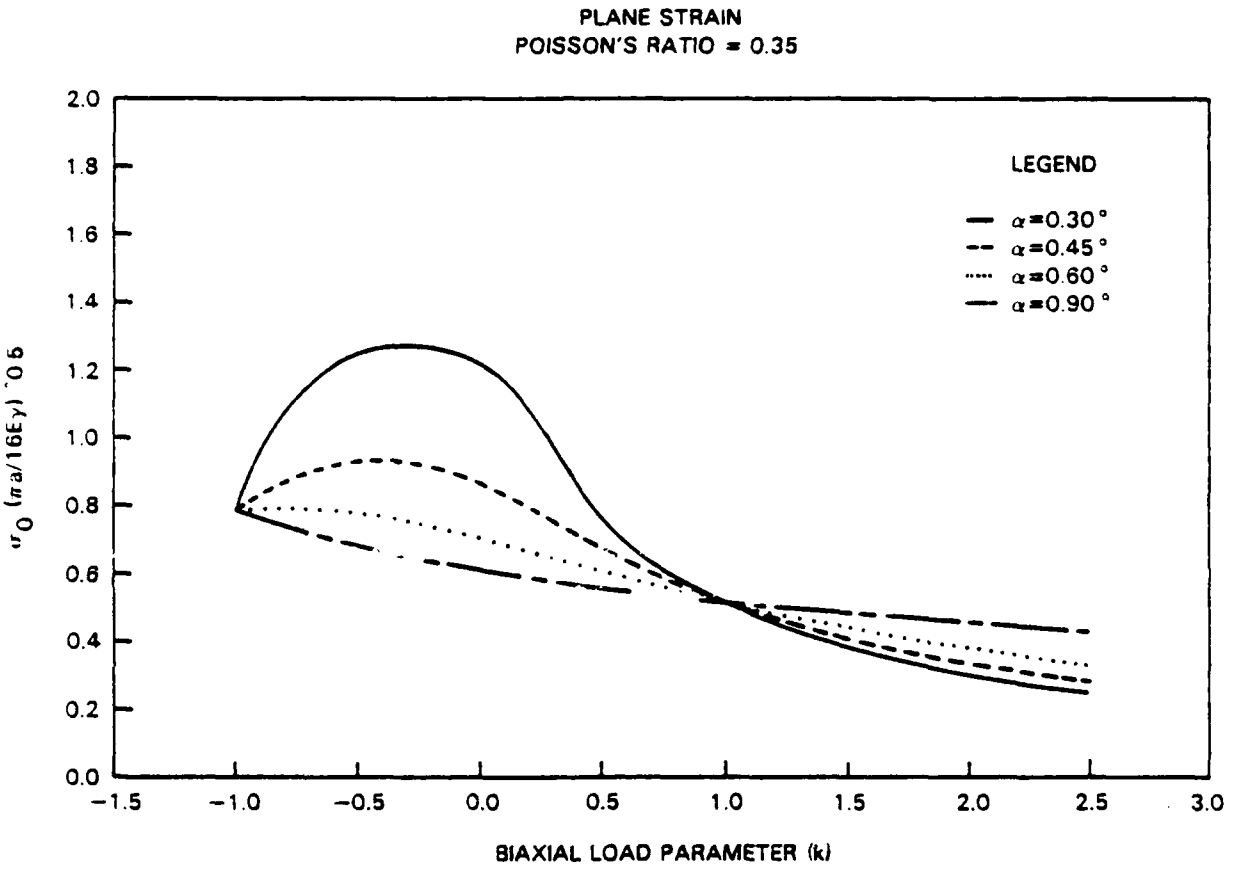

Fig. 16 — Fracture load versus load biaxiality.

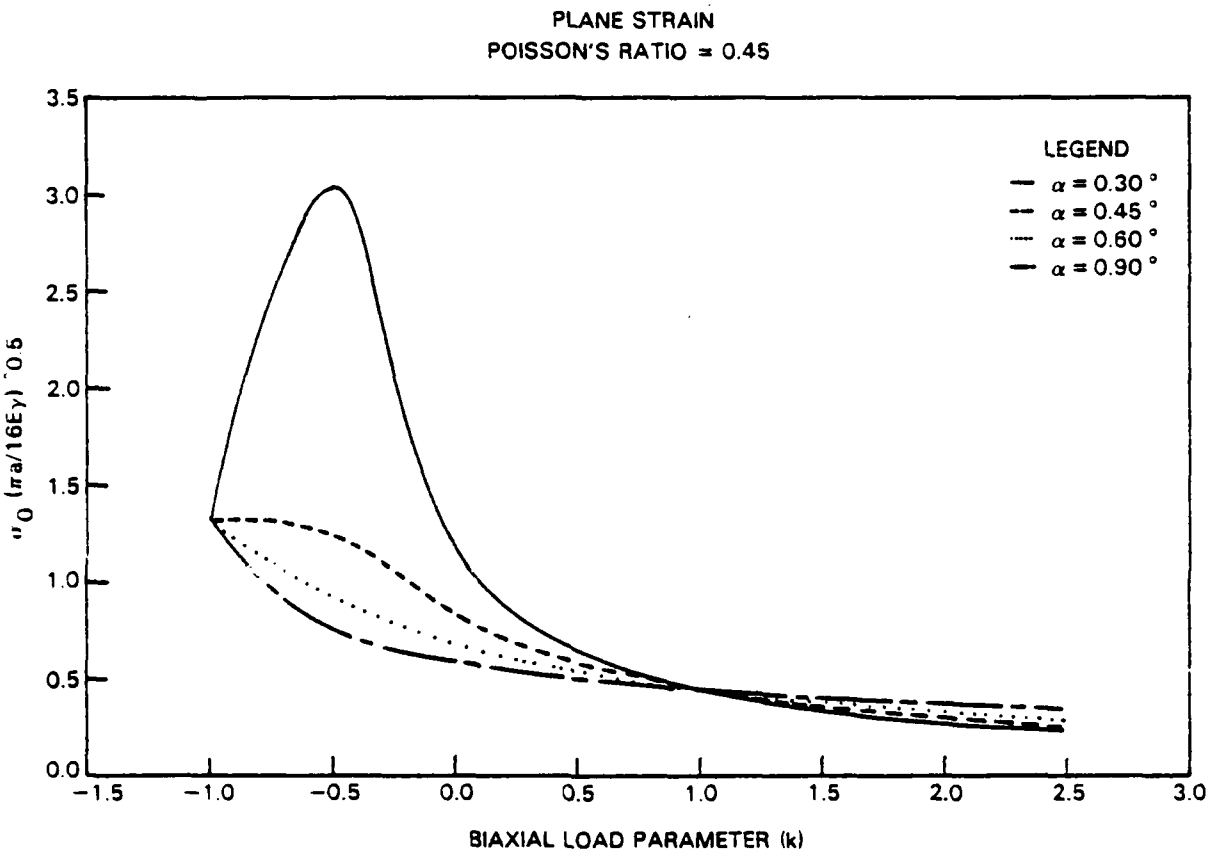

Fig. 17 — Fracture load versus load biaxiality.

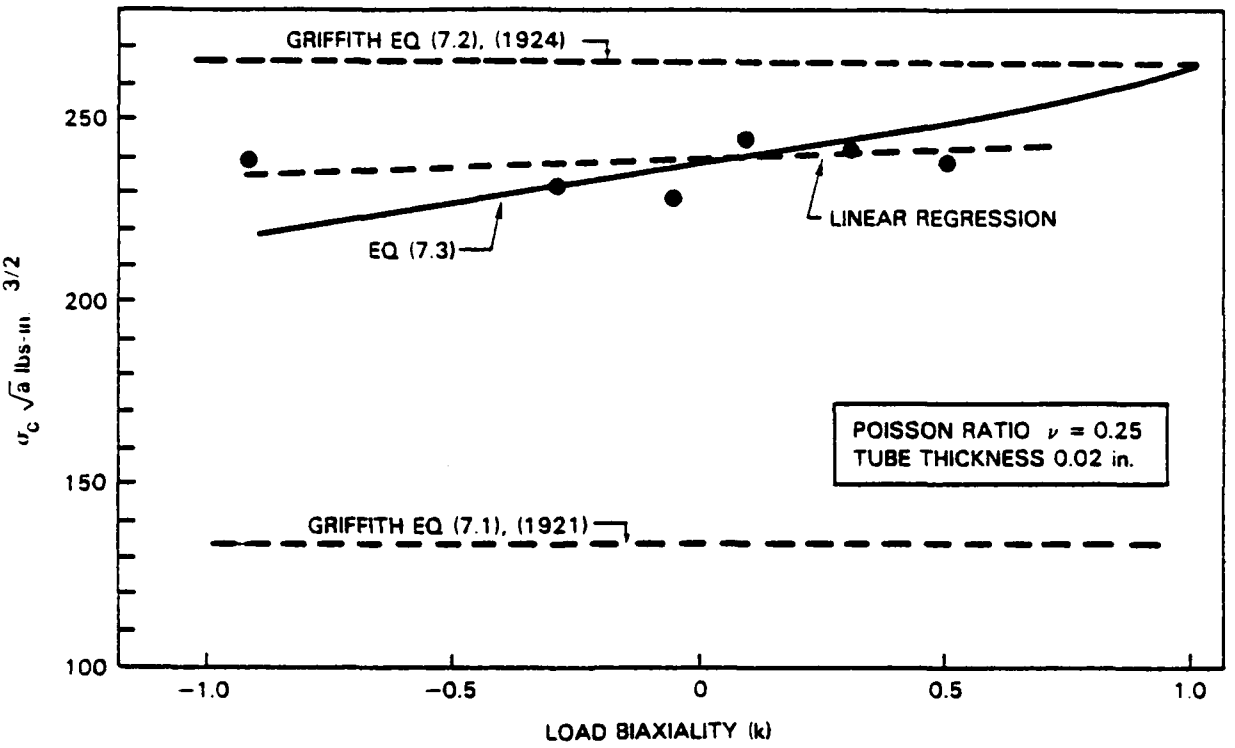

Fig. 18 — Fracture load for Glass—plane stress.
(Griffith's glass tube fracture tests)

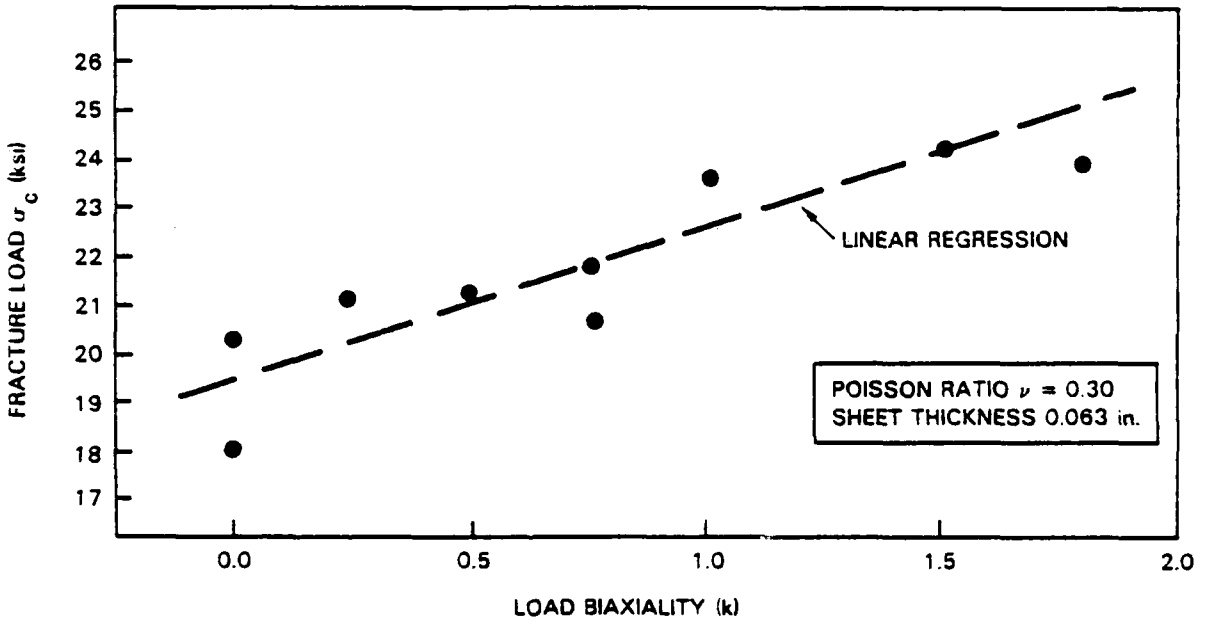

Fig. 19 — Fracture load for Alum. Alloy 7075-T6—plane stress. Crack parallel to the roll direction. (George Washington Univ. tests)

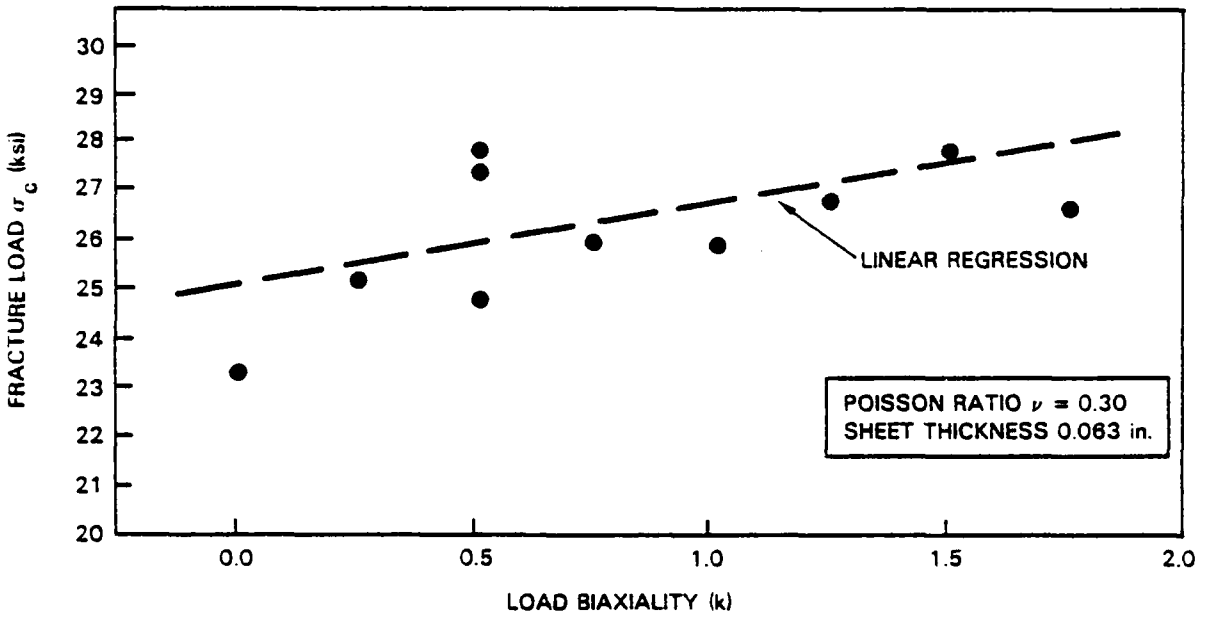

Fig. 20 — Fracture load for Alum. Alloy 7075-T6—plane stress.
Crack perpendicular to the roll direction. (George Washington Univ. tests)

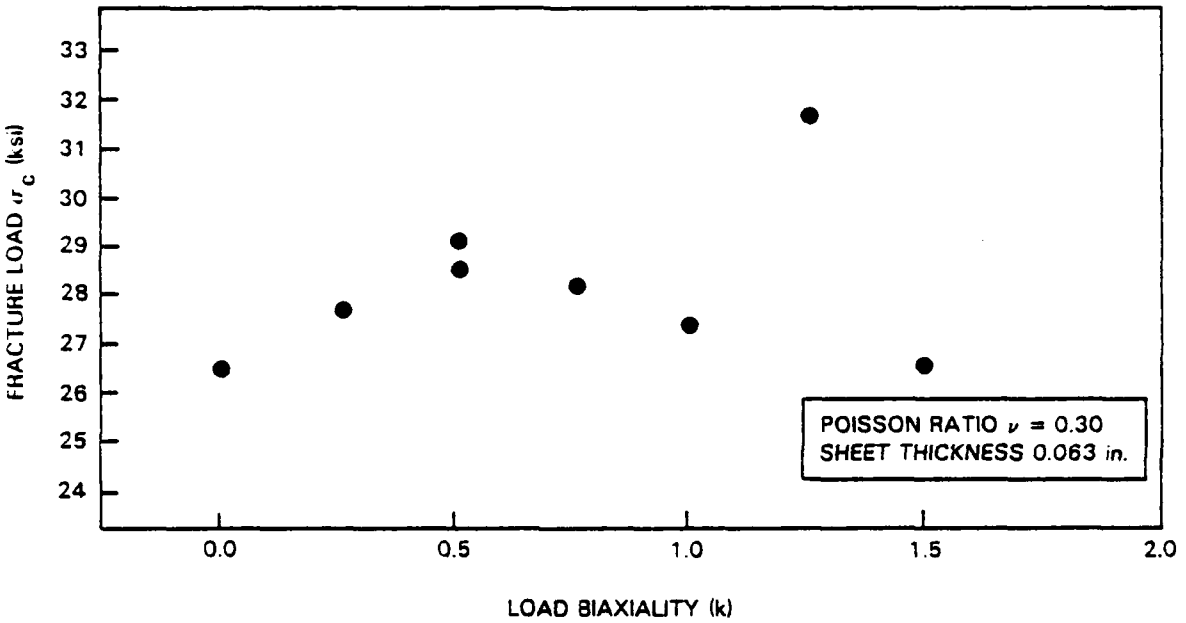

Fig. 21 — Fracture load for Alum. Alloy 2024-T3—plane stress.
Crack perpendicular to the roll direction. (George Washington Univ. tests)

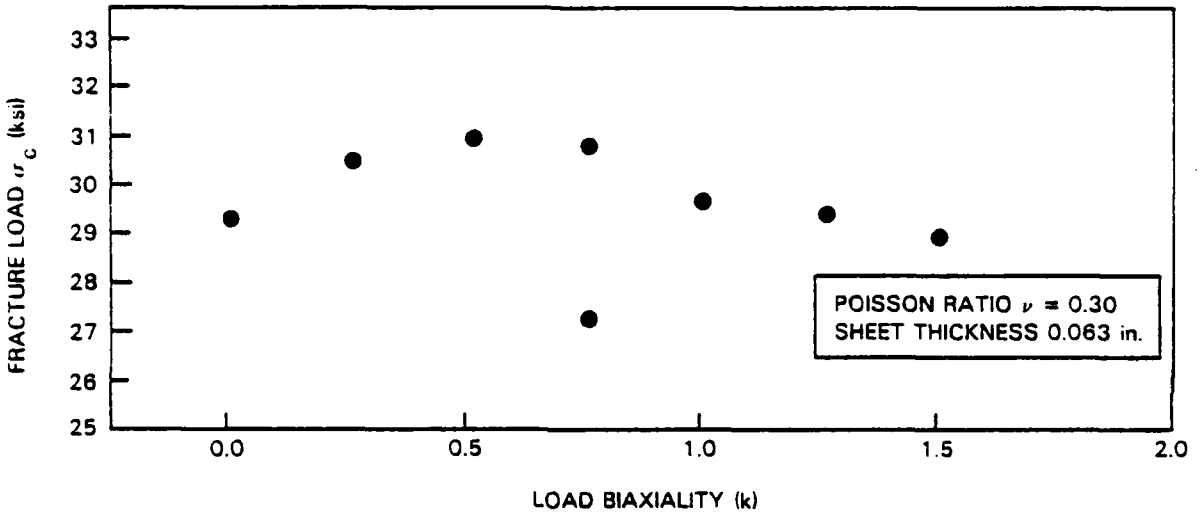

Fig. 22 — Fracture load for Alum. Alloy 2024-T3—plane stress. Crack parallel to the roll direction. (George Washington Univ. tests)

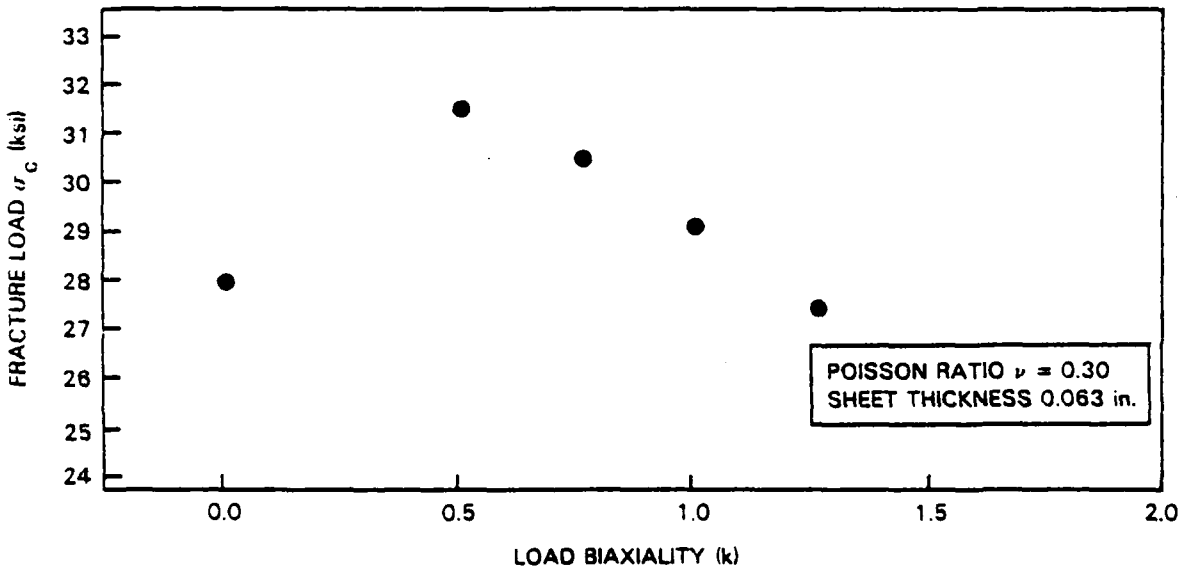

Fig. 23 — Fracture load for Alum. Alloy 6061-T4—plane stress.
Crack perpendicular to the roll direction. (George Washington Univ. tests)

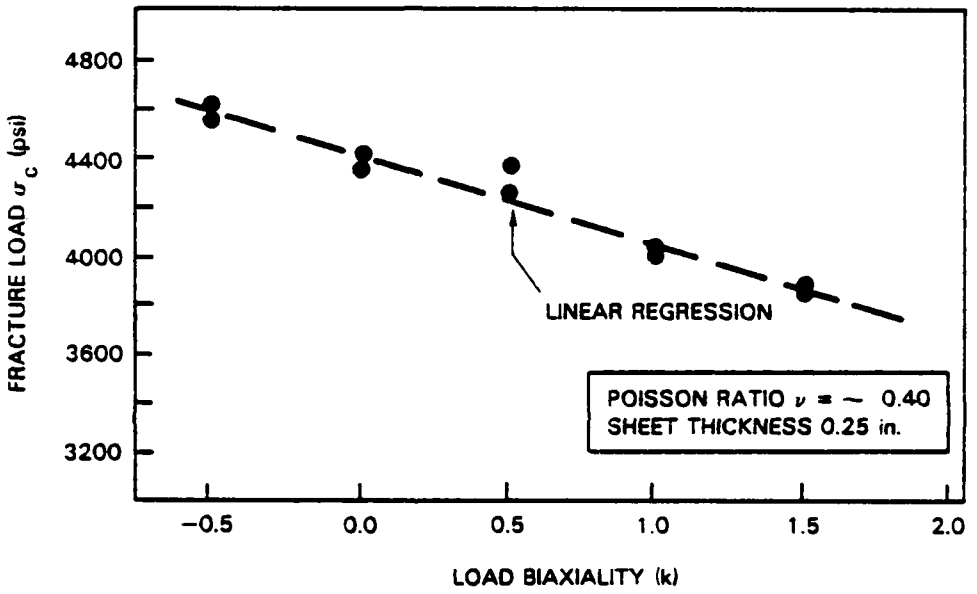

Fig. 24 — Fracture load for PVC—plane strain.
(George Washington Univ. tests)

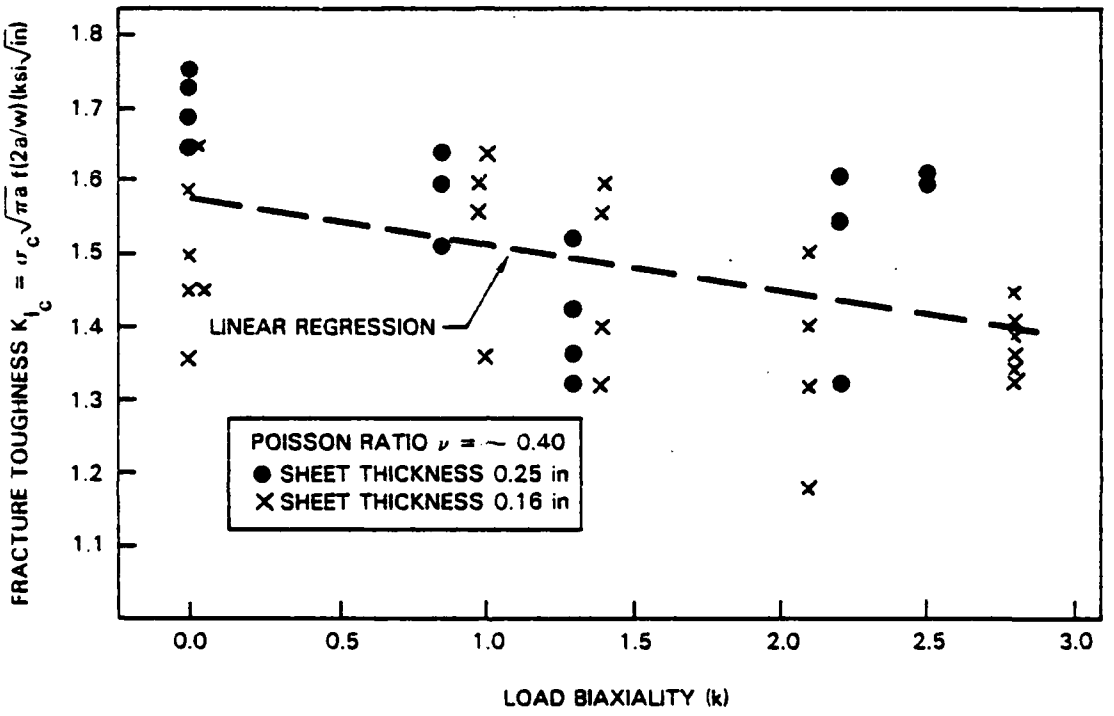

Fig. 25 — Fracture toughness for PMMA—plane strain.
(Imperial College of Technology tests)

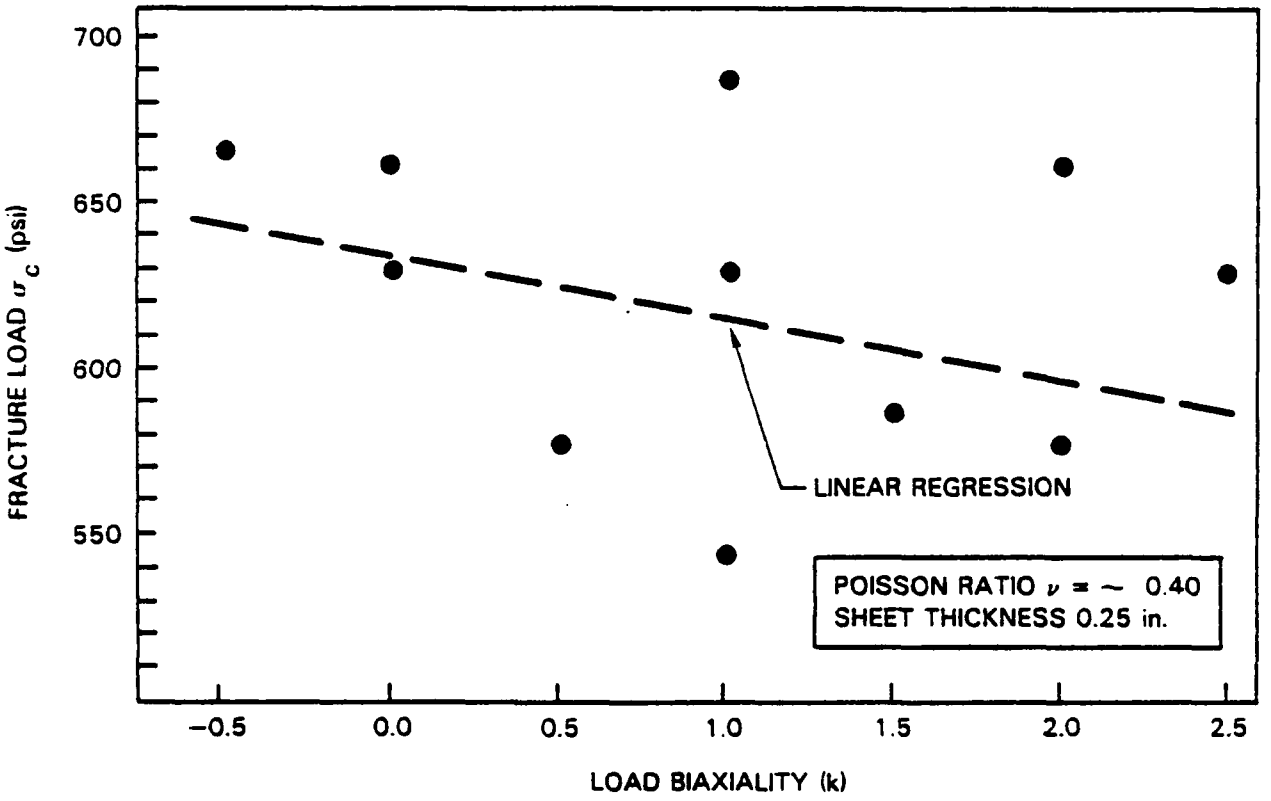

Fig. 26 — Fracture load for PMMA—plane strain.
(George Washington Univ. tests)

END

2-87

DTIC